Nonlinear Free Energy Relations for Adiabatic Proton Transfer Reactions in a Polar Environment. I. Fixed Proton Donor−Acceptor Separation

Philip M. Kiefer[†] and James T. Hynes*[,†,‡]

Department of Chemistry and Biochemistry, University of Colorado, Boulder, Colorado 80309-0215 and Département de Chimie, CNRS UMR 8640 PASTEUR, Ecole Normale Supérieure, 24, rue Lhomond, 75231 Paris, France

Received: September 6, 2001; In Final Form: December 18, 2001

A quadratic free energy relationship (FER) between the kinetic activation free energy $\Delta G^{\ddagger}$ and the thermodynamic reaction asymmetry ΔG_{RXN} is derived for acid-base ionization proton-transfer reactions $AH\cdots B \rightarrow A^{-}\cdots HB^{+}$ in a polar environment in the proton adiabatic regime, in which the proton is treated quantum mechanically, but does not tunnel. The description differs from traditional treatments in both the proton quantization and the identification of a solvent coordinate as the reaction coordinate. The key coefficients in the FER are analyzed analytically for the simplified case, where the proton donor−acceptor distance is held fixed (a restriction removed in the following paper). In particular, the intrinsic barrier is shown to be the sum of an intrinsic solvent barrier, largely determined by solvent reorganization, and the zero point energy difference of the proton between the reactant and the transition state in a solvent coordinate. The Brønsted coefficient is related to the quantum proton-averaged solute electronic structure at, and the position of, this transition state along this reaction coordinate. Similarities and differences of the FER with the well-known Marcus relation are discussed.

1. Introduction

Proton transfer (PT) reactions are of obvious central importance in both chemistry and biology,[1] and accordingly, there has been intensive study of PT rates in solution and other polar environments, e.g., proteins.[1−4] Of particular importance in both comprehending and characterizing PT reactions is understanding rate, equilibrium free energy relations connecting the activation free energy $\Delta G^{\ddagger}$ of the reaction with the thermodynamic reaction asymmetry ΔG_{RXN}. The quantitative nature of this trend has been modeled by several workers;[2,3,5−9] of special interest is the nonlinear free energy relation (FER) introduced by Marcus[5]

$$\Delta G^{\ddagger} = \Delta G_{o}^{\ddagger} + \frac{\Delta G_{RXN}}{2} + \frac{(\Delta G_{RXN})^{2}}{16\Delta G_{o}^{\ddagger}} \qquad (1.1)$$

where $\Delta G_{o}^{\ddagger}$ is the "intrinsic" reaction barrier ($\Delta G_{o}^{\ddagger} = \Delta G^{\ddagger}$-($\Delta G_{RXN} = 0$)), i.e., the activation free energy for the reference thermodynamically symmetric reaction. This relation has had impressive success in correlating solution phase and other PT reaction data,[2a−d,4,5] but it is important to appreciate that this Marcus relation was never actually derived for PT reactions.[10] An FER was initially derived by Marcus[5] for a gas phase H transfer situation using a bond energy-bond order (BEBO) relationship, and independently the relation eq 1.1—originally derived by Marcus for outer sphere electron-transfer reactions in solution[11]—was posited because it gave a FER similar to that resulting from the BEBO analysis. However, neither of these physical models individually is a plausible model for PT, which simultaneously involves bond breaking and making as well as strong electrostatic reacting solute-surrounding solvent interaction. Several researchers[3,6] have stressed the importance of understanding how an equation whose structure is based on electron transfer (ET) theory could be successful in the PT context, where the assumptions of ET theory do not apply. For example, ET theory generally assumes that the electronic coupling between reactant and product states is small, say a kcal/mol or even less,[11] whereas for PT, a typical electronic coupling value is of the order of an electronvolt,[9,12,13] a feature reflecting the absence of bond breaking/making in outer sphere ET but its essential presence in PT. (This aspect is appreciated in some work[5d] but not in other efforts.[14]) One goal of the present work is to show how a second-order FER similar to the Marcus eq 1.1 emerges, using a simplified but realistic theoretical treatment of PT reactions in a polar medium. Beyond this, the analysis also (a) characterizes the intrinsic reaction free energy barrier—which is typically (though not always[15]) regarded as a parameter in correlating PT rates and equilibria—in terms of fundamental molecular and solvation features, and (b) forms the basis for a nonconventional theoretical perspective for kinetic isotope effects.[16]

The underlying picture of PT reactions[7,8,12,17,18] employed within differs considerably from "standard" approaches.[1,4,19] For example, the reaction is driven by configurational changes in the surrounding polar environment—a feature of much modern work on PT reactions[7−9,12,13,17,18,20−28]—and the reaction activation free energy is largely determined by the reorganization of this environment, rather than directly by the height of any potential barrier in the transferring proton's coordinate, the latter being the focus of traditional approaches.[29] In this picture, the rapidly vibrating proton adiabatically follows the slower rearrangement of the environment,[7,8,17,18] and one focuses on the instantaneous proton potential for different environmental arrangements. Figure 1 illustrates this nonequilibrium solvent

* To whom correspondence should be sent.
[†] Department of Chemistry and Biochemistry, University of Colorado.
[‡] Département de Chimie, CNRS UMR 8640 PASTEUR, Ecole Normale Supérieure.

10.1021/jp0134244 CCC: $22.00
Published on Web 02/08/2002

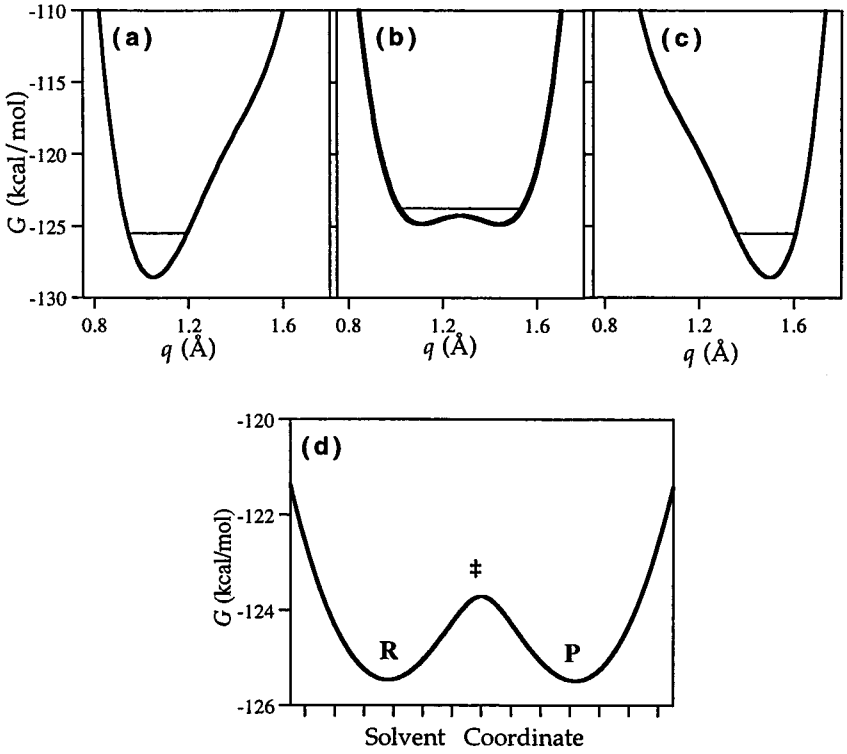

Figure 1. Free energy curves versus proton position q for fixed proton donor−acceptor separation $Q = 2.55$ Å and at (a) the reactant, (b) transition state and (c) product state solvent configurations. In each case, the ground-state proton vibrational energy level is indicated. (d) Free energy of the PT system, with the proton quantized in its vibrational ground state, versus solvent reaction coordinate. The solvent coordinate critical points corresponding to the proton potentials in panels (a)−(c) are indicated.

assisted PT view. Figure 1a−1c displays the system free energy curves as a function of the proton coordinate with the ground proton vibrational state indicated, for three values of the solvent coordinate characterizing different environmental configurations. As depicted, evolution in the solvent coordinate (defined precisely within) leads to an evolving proton potential pattern, in which the proton is initially bound to a donor in the reactant state (Figure 1a), to a transition state with the proton delocalized to a degree between donor and acceptor moieties (Figure 1b), and finally to the product state with the proton bound to the acceptor (Figure 1c). The evolving zero point vibrational energy of the proton, which includes its interaction with the environment, defines a free energy as a function of the environment rearrangement, shown in Figure 1d. The labels R, ‡, and P in Figure 1d correspond to the reactant, product, and transition states along the reaction coordinate, and correspond to the ground proton vibrational energy levels displayed in Figure 1a−1c. The reaction barrier is thus in the solvent coordinate, as opposed to the proton coordinate in the "standard" picture. At the transition state solvent configuration (for a thermodynamically symmetric reaction), the proton potential is a symmetric double well.

Figure 1 depicts what we term the *proton adiabatic* regime, in which the quantized proton vibrational level lies above the proton barrier at the environment's transition state (TS) configuration.[22] This adiabatic PT regime picture has been supported in electronic structure/simulation studies including acid ionizations in solution[17] and elsewhere.[18,24] The TS for adiabatic PT situation described above corresponds to what has been termed in the enzyme reaction literature a "low barrier hydrogen bond".[30] As discussed below in more detail, the adiabatic proton regime is expected to apply for proton donor/acceptor systems in which there is a hydrogen bond (H-bond) of sufficient strength. We stress that the proton motion is a bound quantized vibration here, rather than a classical, over the barrier, motion as in standard approaches. A separate and distinct quantum regime—*nonadiabatic* PT or tunneling[7,8,18,20,21,23,25−27]—occurs if the zero point vibrational energy in the TS proton potential is below the central proton barrier top. FERs for nonadiabatic PT in this picture have been presented in ref 7 (see also ref 8).

The above description has ignored, for simplicity, the important influence of the separation between the heavy donor and acceptor moieties between which the proton is transferred. This H-bond coordinate's most salient aspect is its influence on the proton barrier (Figure 1b) at the environment's TS configuration: this barrier will increase as the donor−acceptor separation is increased; a higher energetic price must be paid in breaking the original bond before the energetic gain from the new bond formation is realized. The PT reaction must thus be considered not only in the presence of a barrier whose asymmetry is fluctuating due to the environment, but one whose height (and width) is also fluctuating. Figure 2 shows such a barrier height increase as the donor−acceptor distance increases, going from Figure 2a to 2b, with the proton adiabatic condition maintained. For perspective, Figure 2c displays an extreme case: the H-bond separation is sufficiently large that the ground-state proton vibrational energy level is no longer above the proton coordinate barrier; this is nonadiabatic PT—tunneling—and is excluded in the present work. Nonetheless, Figure 2c emphasizes that attention must be paid that the system remains adiabatic; in this work, we require sufficient H-bond strength to ensure small equilibrium separations in the reactant H-bonded complex.

The outline of the remainder of this paper is the following. Section 2 discusses the theoretical formalism used to evaluate the free energy surface from which barrier heights and reaction free energies will be analyzed, whereas section 3 presents the parametrization and specification of model potentials used to

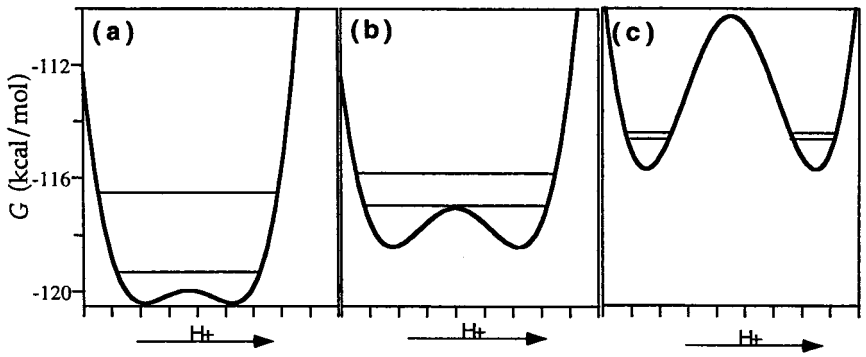

Figure 2. Variation of the reaction transition state proton potentials with increasing H-bond coordinate AB separation, going from (a) to (c). Both the ground and the first excited proton vibrational levels are indicated.

illustrate the formalism of section 2. The free energy relationship is analyzed in general terms in section 4, with detailed derivation of its specifics described in section 5. Concluding remarks are offered in section 6. Beginning with section 4, we restrict the discussion to a fixed donor−acceptor separation, a restriction removed in the following paper,[31] hereafter labeled II; as will be seen there, the basic structure remains the same.

2. Theoretical Formalism for the Reaction Free Energy Surface

We introduce a simplified model system for an acid ionization PT to calculate the free energy surface from which the free energy barrier and reaction asymmetry can be extracted. The model consists of PT between a donor, A, and acceptor, B, separated by the H-bond distance Q, with q the proton−donor separation, in short, the proton coordinate

$$\mathrm{AH\cdots B} \rightleftharpoons \mathrm{A^-\cdots HB^+} \tag{2.1}$$

We will be concerned only with the "chemical" aspect of the PT reaction, i.e., that portion occurring within a hydrogen-bonded complex to produce a contact ion pair product complex.[32] The system gas-phase electronic Hamiltonian is constructed in terms of a two valence bond (VB) state picture. These two electronic VB states correspond to a neutral and an ion pair, as suggested in eq 2.1, and are defined at each value of the q and Q coordinates. This description has its foundation in the Mulliken charge-transfer picture[33] of PT, in which an electron is transferred from a nonbonding orbital (e.g., lone pair) on the (proton acceptor) base to the antibonding orbital of the (proton donating) acid. The A−H bond accordingly weakens and a hydrogenic species can move from A to B. This somewhat nonconventional picture has now been supported by several ab initio calculations for acid ionization[17] and elsewhere,[24] which show that the transferring species actually carries a fraction of the charge of a proton; we will nonetheless continue to refer to "proton transfer" throughout.

The basic formulation of the PT system free energy surface in this two VB state framework was developed in ref 12, where discussion of its antecedents, including work of e.g., Coulson, Bratos, and Warshel[9,34] may be found. We summarize only the essential features from that work here. First, the gas phase Hamiltonian at each solute geometry is a two-dimensional matrix for the neutral (N) and ionic (I) VB states with an off -diagonal electronic coupling element mixing them to produce the electronically adiabatic states

$$\hat{H}_{\mathrm{vac}} = \begin{bmatrix} U_{\mathrm{N}} & -\beta \\ -\beta & U_{\mathrm{I}} + \Delta_{\mathrm{vac}} \end{bmatrix} \tag{2.2}$$

We will only be concerned with the *ground* electronically adiabatic state produced by the electronic, or resonance coupling $-\beta$, and this choice will be taken in all that follows. In eq 2.2, U_{N} and U_{I} are the two electronically diabatic VB state gas-phase surfaces. It proves convenient to have the same zero of energy for U_{N} and U_{I}, so that Δ_{vac} explicitly indicates the gas-phase offset between the reactant and product diabatic states, and thus represents the gas-phase transfer reaction asymmetry (without any zero point energy effects, vide infra).

In the above two diabatic state representation, the ground adiabatic electronic wave function is the linear combination

$$|\Psi\rangle = c_{\mathrm{N}}|\Psi_{\mathrm{N}}\rangle + c_{\mathrm{I}}|\Psi_{\mathrm{I}}\rangle \tag{2.3}$$

where the coefficients c_{N} and c_{I} describe the solute's electronic composition in terms of the neutral and ionic VB state wave functions Ψ_{N} and Ψ_{I}. In this representation, the gas-phase ground adiabatic electronic energy is the expectation value

$$\langle \hat{H}_{\mathrm{vac}} \rangle = \langle \Psi | \hat{H}_{\mathrm{vac}} | \Psi \rangle = c_{\mathrm{N}}^2 U_{\mathrm{N}} + c_{\mathrm{I}}^2 U_{\mathrm{I}} - 2c_{\mathrm{I}}c_{\mathrm{N}}\beta \tag{2.4}$$

After these gas-phase preliminaries, we turn to the situation of interest, in which the solute system is immersed in a polar solvent, mimicked as a dielectric continuum with static (ϵ_o) and optical (ϵ_∞) dielectric constants. As seen within, we will couch our general final results in a form that should apply beyond such a description. The solute−solvent interaction is modeled in the point dipole approximation for the solute charge distribution; each diabatic state is characterized by its own dipole moment (μ_{N} and μ_{I}), which together with a transition dipole moment μ_{NI}, determine the expectation value of the dipole moment $\hat{\mu}$ in the solute electronic state Ψ

$$\langle \mu \rangle = \langle \Psi | \hat{\mu} | \Psi \rangle = c_{\mathrm{N}}^2 \mu_{\mathrm{N}} + c_{\mathrm{I}}^2 \mu_{\mathrm{I}} + 2c_{\mathrm{N}}c_{\mathrm{I}}\mu_{\mathrm{NI}}; \hat{\mu} = \begin{bmatrix} \mu_N & \mu_{NI} \\ \mu_{NI} & \mu_I \end{bmatrix} \tag{2.5}$$

In general, the solvent electronic polarization is equilibrated to a certain mixture of VB states which must be self-consistently determined.[35] Here, we will consider for simplicity the Born−Oppenheimer (BO) limit[35] in which the fast solvent electronic polarization is equilibrated to the individual VB states,[36] and in which the system nonequilibrium free energy is described by[12]

$$G_{\mathrm{q}} = \langle \hat{H}_{\mathrm{vac}} \rangle + K[-z\langle \hat{\mu} \rangle + {}^1/_2 z^2] - {}^1/_2 K_\infty \langle \hat{\mu}^2 \rangle \tag{2.6}$$

with expectation values taken over the solute electronic wave function. The first three terms in eq 2.6 are respectively the solute's gas-phase energy at the solute's solution phase elec-

tronic structure, the solute−solvent interaction energy, and the solvent's self-free energy. The last term is the stabilization free energy due to the solvent electronic polarization. The notation G_q indicates explicit dependence of the free energy on the proton coordinate q, to distinguish it from a free energy subsequently introduced, in which the proton motion is quantized.

In eq 2.6, z is a coordinate describing the solvent orientational polarization, and corresponds to the solute dipole moment that the solvent configuration would be equilibrated with *if* there were equilibrium solvation. Because z can in fact differ from $\langle\hat{\mu}\rangle$, the system can be out of equilibrium, an essential feature of the description; the solvent polarization state is whatever it happens to be, and is not necessarily that polarization which is equilibrated to the PT solute system's actual charge distribution. The force constants for the orientational and electronic polarization of the solvent

$$K = 2M_S\left(\frac{1}{\epsilon_\infty} - \frac{1}{\epsilon_o}\right); K_\infty = 2M_S\left(1 - \frac{1}{\epsilon_\infty}\right) \qquad (2.7)$$

depend on the static and optical dielectric constants, as well as a structure factor, M_s, discussed later.

The quadratic dependence on the solvent coordinate z in eq 2.6 results from nonequilibrium fluctuation of the environment's polarization around its equilibrium position. A solvent polarization coordinate was first introduced in reaction dynamics for outer sphere ET by Marcus,[11] with a resulting quadratic dependence of the free energy on the polarization of the medium. (For more complex charge transfers in a polar environment, theories have been developed which also include the solvent polarization−solute charge distribution interaction; examples include PT[7−9,12,13,17,18,20,22,23,27] and other[12,35,37] reactions.) But as will be seen, the quadratic dependence of G in eq 2.6 for the PT case does not at all guarantee a quadratic FER as in eq 1.1.

The solute's electronic composition, defined by the coefficients c_N and c_I, is determined by solution of the generalized Schrödinger equation

$$\{\hat{H}_{vac} - Kz\hat{\mu} - {}^1/_2K_\infty\hat{\mu}^2 - E\mathbf{1}\}\begin{bmatrix}c_N\\c_I\end{bmatrix} = 0$$

where E is the ground adiabatic energy eigenvalue for the matrix

$$\hat{H} = \begin{pmatrix}U_N - K\mu_N z - {}^1/_2K_\infty\mu_N^2 & -\beta'\\ -\beta' & U_I - K\mu_I z - {}^1/_2K_\infty\mu_I^2 + \Delta_{vac}\end{pmatrix} \qquad (2.8)$$

The off-diagonal term in the Hamiltonian contains the renormalized electronic coupling $-\beta'$, which includes the solvent contribution to the resonance coupling,[12,35] $-\beta' = -\beta - K\mu_{NI}z - {}^1/_2K_\infty\mu_{NI}(\mu_N + \mu_I)$.

It is convenient to replace the coordinate z with a different, linearly related solvent coordinate, ΔE, the offset between the electronically diabatic states which is modulated by the solvent

$$\Delta E = -\Delta_{vac} - K(\mu_N - \mu_I)z - {}^1/_2K_\infty(\mu_N^2 - \mu_I^2) \qquad (2.9)$$

$\Delta E = 0$ corresponds to zero offset between the two diabatic proton potentials, and to a symmetric proton potential in q. The algebraic sign of ΔE is defined such that $\Delta E < 0$ corresponds to the reactant region, i.e., solvent configurations close to those appropriate to equilibrium solvation of the solute in its reactant configuration, and $\Delta E > 0$ corresponds to the product region. ΔE is similar to the solvent reaction coordinate typically used for ET[38] and more recently PT[9,17,18,20,24,27] reactions in which simulation techniques are employed to calculate free energy surfaces. For a given ΔE and nuclear configuration, the coefficients c_N and c_I can be obtained by solving the generalized Schrödinger equation, eq 2.8. The free energy is calculated from eq 2.6, with the expectation values evaluated with c_I and c_N, and from eqs 2.6−2.9, the free energy G_q is

$$G_q(q;\Delta E) = \frac{1}{2K(\mu_N - \mu_I)^2}(\Delta G_d + \Delta E)^2 - \frac{K}{2}\left(\frac{\mu_N + \mu_I}{2}\right)^2 - \frac{K_\infty}{2}\left(\frac{\mu_N^2 + \mu_I^2}{2}\right) + \frac{\Delta_{vac}}{2} + \frac{U_N + U_I}{2} - \frac{1}{2}\sqrt{(U_N - U_I + \Delta E)^2 + 4\beta'^2} \qquad (2.10)$$

and the VB coefficients are given by

$$c_I^2 = \frac{1}{2} + \frac{1}{2}\frac{(\Delta E + U_N - U_I)}{\sqrt{(\Delta E + U_N - U_I)^2 + 4\beta'^2}}; c_N^2 + c_I^2 = 1 \qquad (2.11)$$

We have also introduced in eq 2.10 the difference in free energy between the equilibrium solvated ionic and the neutral diabatic electronic states as the sum of the gas-phase offset and the difference in solvation free energy between those states

$$\Delta G_d = \Delta_{vac} + {}^1/_2(K + K_\infty)(\mu_N^2 - \mu_I^2) \qquad (2.12)$$

Equation 2.10 defines the system free energy as a function of the three coordinates, and illustrations of this surface versus q for a fixed H-bond coordinate Q and at several different ΔE values were given in Figure 1a−1c. We now introduce the quantization of the nuclear proton motion. Because this motion is typically fast compared to that of the solvent and the AB vibration (vide infra), a Born−Oppenheimer approximation is made for the proton with respect to these two coordinates; proton motion is quantized by solving the nuclear Schrödinger equation for the proton Hamiltonian at each Q and ΔE

$$\hat{H}_q|\phi_{q,v}\rangle = \{\hat{K}_q + G_q(q;Q,\Delta E)\}|\phi_{q,v}\rangle = G_v(Q,\Delta E)|\phi_{q,v}\rangle \qquad (2.13)$$

Here, $\hat{K}_q$ is the proton's kinetic energy operator and $G_q(q;Q,\Delta E)$ is the effective potential seen by the proton at each ΔE and Q. The result is a set of proton vibrational energy levels $G_v(Q,\Delta E)$, together with the associated proton vibrational wave functions $\phi_{q,v}$, with examples shown in Figures 1 and 2.[39] With some exceptions,[7d,16,23a] dealt with elsewhere,[16] the proton will usually reside in its ground-state vibrational level, i.e., the proton vibrational energy is then closely related to the zero point energy (ZPE). Thus, the resultant free energy surface after proton quantization, $G_{v=0}(Q,\Delta E)$, contains the proton ZPE in addition to the solvent self-free energy and the solute−solvent interaction free energy; hereafter, we suppress the notation "v=0", for convenience.

Then, following ref 24, G can be most revealingly decomposed into the two components

$$G(Q,\Delta E) = G_{min}(Q,\Delta E) + ZPE(Q,\Delta E) \qquad (2.14)$$

This key equation provides our basic picture. Here, G_{min} is the system free energy with the proton *fixed* at its classical mechanical equilibrium position, located at the minimum of the

proton potential defined by a specific Q and ΔE, e.g., the minima in Figure 1a−1c, whereas ZPE is the quantum zero point energy of proton vibration, defined at any given Q and ΔE as the difference in energy between the proton vibrational ground-state energy and the proton potential minimum.

3. Model Parameters

In this section, we pause to describe the various model specifications used subsequently to illustrate the formalism of section 2.

3a. Valence Bond State Potentials. Each electronic diabatic state potential energy, U_N and U_I, is assumed to have a simple form

$$U_N = V_N(q) + V_Q(Q);\ U_I = V_I(Q - q) + V_Q(Q) \quad (3.1)$$

Here, V_N and V_I describe the bonding interaction between the proton and donor or acceptor, respectively. Both are taken to be Morse potentials ($(V_M(q) = D\{\exp[-2a_m(q - q_o)] - 2\exp[-a_m(q - q_o)]\}$) with identical interactions (the same D, a_m, and q_o), except that different bonding partners for the proton are described: $V_N(q) = V_M(q)$ and $V_I(Q - q) = V_M(Q - q)$.[40] We add to each valence bond potential an AB interaction potential, $V_Q(Q)$, further specified below, which describes the A−B repulsive and electrostatic interactions within the H-bond.

In the present work, we will take the majority of the numerical parameters characterizing the reacting solute system as those appropriate for PT between oxygen atoms. The Morse potential dissociation energy, D, is taken to be that of a typical hydroxyl O−H bond, $D = 5$ eV $= 115.3$ kcal/mol. The length parameter a_m is determined by the OH stretch frequency appropriate for an H-bond at a given O···O separation.[41] For an equilibrium H-bond separation $Q = 2.55$ Å, the OH frequency is ∼2650 cm^{-1} with a corresponding equilibrium proton position ∼ 1 Å;[28,41] then $a_m = 1.67$ Å^{-1} and $q_o = 1.02$ Å. We take identical Morse potentials for the proton donor -acceptor interactions, and identical donor and acceptor nuclei, namely oxygen atoms. One could instead use differing Morse potential parameters, which would add a ZPE contribution to the reaction asymmetry, an aspect which will be discussed elsewhere.[42] In our model treatment, the reaction asymmetry in solution arises only from the gas-phase offset Δ_{vac} between U_N and U_I (See eq 2.2), and the difference in solvation free energy between the solvated reactant and product states. The variation of Δ_{vac} can be thought of as e.g., changing the electron withdrawing capacity of substituents on the donor or acceptor, leading to a ΔpK_a between the donor and acceptor.

The vacuum electronic resonance coupling, β, is a function of both nuclear coordinates q and Q. The variation with respect to the proton position q is, however, generally small[7a,12] and is ignored here. On the other hand, β varies strongly—approximately exponentially[12,43]—with the H-bond stretch, Q. For the present model, we use an exponential form with a previous model PT system's parameters:[12] $\beta = \beta_o \exp(-\beta_Q(Q - Q_o))$ where $\beta_o =$ 35 kcal/mol, $b_Q = 1.5$ Å^{-1}, and $Q_o = 2.55$ Å.

After proton quantization, the Hamiltonian defining the AB motion is

$$\hat{H}_Q = \hat{K}_Q + G(Q,\Delta E) \quad (3.2)$$

where $\hat{K}_Q$ is the Q vibrational mode kinetic energy operator and $G(Q,\Delta E)$ is the ground-state energy of the proton vibrational mode at a given Q and ΔE determined from eq 2.13. The H-bond vibrational potential $V_Q(Q)$ (cf. eq 3.1) includes repulsion and electrostatic attraction between A and B, resulting in a weakly attractive potential, modeled here by a Morse potential, $V_Q(Q) = D_Q(\exp(-2a_Q(Q - Q_o)) - 2\exp(-a_Q(Q - Q_o)))$. The parameters $D_Q = 3.93$ kcal/mol, $a_Q = 2.33$ Å^{-1}, and $Q_o = 2.96$ Å are chosen such that, after proton quantization, the H-bond vibration in the reactant region, described by $G(Q,\Delta E)$ at a representative reactant solvent configuration, has a frequency ∼300 cm^{-1} and a dissociation energy ∼10 kcal/mol, representative values for modest strength H-bonded complexes.[41,45]

3b. Solvent and Solvent Interaction Parameters. The solute−solvent interaction is governed by the reacting solute system diabatic dipole moments, μ_N, μ_I, and μ_{NI}, here chosen to be $\mu_N = 0$, $\mu_I = 12$, and $\mu_{NI} = 0$ Debye, values similar to those of previous studies modeling phenol-amine PT.[17c,46,47] A zero transition moment, $\mu_{NI} = 0$, removes any solvent dependence of the renormalized electronic coupling β'; a finite μ_{NI} causes the resonance coupling to depend on the solvent coordinate ΔE, and would only change the magnitude of β' by ∼30%.[12,35] Hereafter, we take $\beta' = \beta$, which considerably simplifies the analysis without changing the physical picture. The solvent dielectric constants are taken as those of an aqueous environment, $\epsilon_o = 80$ and $\epsilon_\infty = 2$. (Static dielectric constant variation toward less polar solvents, from 80 to 20, will not drastically change K in eq 2.10.) The structure factor M_s in eq 2.7 is set to give an intrinsic barrier for solvent reorganization (∼3 kcal/mol) consistent with PT reactions in an aqueous solution with a similar AB fixed separation[17c] ($M_s = 0.7$ kcal/mol/Debye^2). This solvent barrier and its relationship to the 'intrinsic' reaction barrier $\Delta G_o^{\ddagger}$ will be discussed in section 5.[48]

As noted above, we will vary the reaction asymmetry by varying the gas-phase asymmetry Δ_{vac}. The reaction asymmetry ΔG_{RXN} in solution then arises from both the gas-phase asymmetry Δ_{vac} and the difference in solvation free energy between the solvated reactant and product states, and is quantitatively related to the free energy difference between the reactant and the product diabatic states, ΔG_d in eq 2.12. As will be shown in section 5, the variation in Δ_{vac} has a simple (linear) relationship with the change in ΔG_{RXN}, and thus provides a simple and clear way to vary reaction asymmetry. This avoids a detailed and somewhat arbitrary parametrization—e.g., variation of the valence bond state parameters (e.g., Morse potential parameters and diabatic dipole moments) with Δ_{vac}, whereas capturing the essential features of the asymmetry trends. It is important to note, however, that although the two diabatic state parameters are constant, the ZPEs and the dipole moments for the reactant and product states will *change* with reaction asymmetry, as one would naturally expect, due to the variation in the *adiabatic* electronic structure of the reactant and product states with that asymmetry.

4. PT System Free Energy Results. General Features

4a. General Perspective. Figure 3 is a contour plot of the proton-quantized (ground vibrational state) free energy surface $G(Q, \Delta E)$ for a symmetric reaction generated with the formalism and parameters presented above. The surface exhibits both a reactant and a product well, stable minima each with equilibrium H-bond separations $Q \approx 2.7$ Å. The transition state displayed in Figure 3 is at the surface's saddle point, where $\Delta E = 0$ and $Q \approx 2.5$ Å.

Hereafter, we discuss the PT free energy relations with the simplification of restricting the H-bond AB separation to a fixed value $Q = 2.55$ Å, which is a representative H-bond distance for the PT in Figure 3; we *suppress* the Q notation in all that follows. This simplified fixed Q situation allows discussion of the essential issues without extraneous complications; the

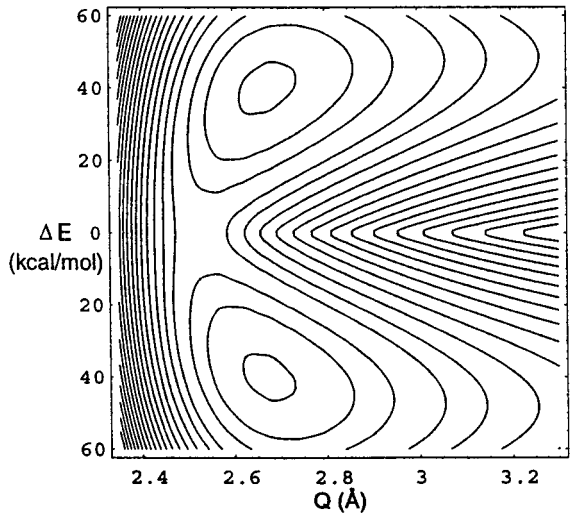

Figure 3. Contour plot of the PT system free energy $G(Q,\Delta E)$ with the proton in its ground vibrational state versus the solvent coordinate, ΔE, and the AB separation, Q, for a symmetric reaction (See section 2 for discussion of the underlying ingredients for this free energy). Contour spacings are set at 1 kcal/mol.

treatment including the H-bond vibration will be given in the companion paper II, where it will be seen that the same basic picture results.

Figure 4a displays a cut of the 3D plot in Figure 3 at $Q = 2.55$ Å, and the solid curve there is the free energy curve for an overall symmetric PT reaction, $\Delta G_{RXN} = 0$. The solid curve in Figure 4b displays the free energy curve for an exothermic reaction, and of course, an endothermic reaction can be viewed as its reverse in Figure 4b. The minima in Figure 4a and 4b define the positions of the reactant, ΔE^R, and product, ΔE^P, states along the solvent coordinate. The reaction free energy is thus $\Delta G_{RXN} = G(\Delta E^P) - G(\Delta E^R)$, with a corresponding equilibrium constant $K_{eq} = \exp(-\Delta G_{RXN}/RT)$. The position of the free energy maximum defines the transition state location for each reaction, $\Delta E^‡$, e.g., the barrier for the forward reaction is $\Delta G^‡ = G(\Delta E^‡) - G(\Delta E^R)$.[49]

The activation barrier values in Figure 4 and elsewhere in this work are low, of the order of several kcal/mol or less, values typical for PT involving O donors and O/N acceptors (without any significant reorganization effects in Q).[1c,17,51,52] This often makes it difficult to experimentally extract rate information on the chemical step for such reactions; but for example, a recent excited electronic state PT study indicates how such difficulties can be overcome, and nonlinear free energy relationships examined.[51]

The solid curves G in Figure 4a and 4b correspond to the free energy curves with the proton in its ground vibrational state. For the dashed free energy curves, denoted G_{min} and defined in eq 2.14, the proton position is fixed at the proton potential minimum for each solvent configuration. The proton ZPE is the difference between G and G_{min} and is displayed in Figure 4c. The electronic adiabatic potential surfaces for the proton from which G_{min}, and the ZPE were extracted for Figure 4 are shown in Figure 1 at the (a) reactant R, (b) transition TS, and (c) product P state solvent configurations indicated in Figure 4a.

The cusp at $\Delta E = 0$ in G_{min} (see Figure 4a and 4b) is a result of a switch in q_{min}, as now described. In the R region, the proton potential minimum is consistently closer to the donor (at $q_{min} \approx 1$ Å), whereas in the P region, it is closer to the acceptor ($q_{min} \approx Q - 1$ Å $\sim$1.5 Å). The proton potential absolute

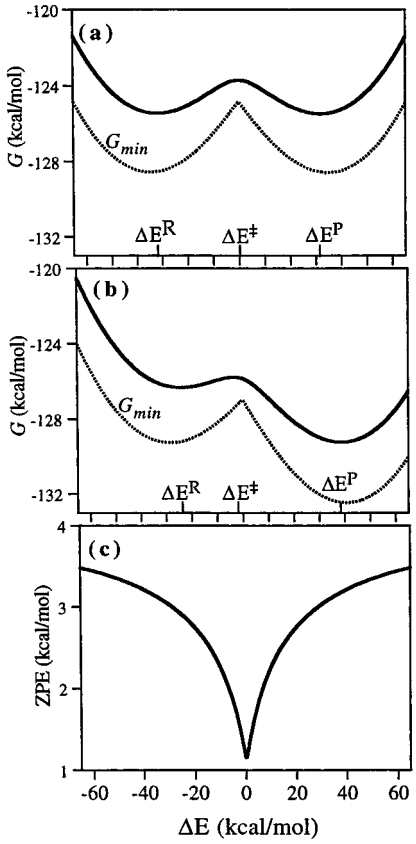

Figure 4. Free energy curves (solid lines) for the proton for fixed AB separation $Q = 2.55$ Å, (a) symmetric reaction and (b) asymmetric reaction. Dashed lines show the free energy curves G_{min} excluding the proton zero point energy (ZPE). (c) ZPE for the proton vs ΔE. The addition of the dashed curves G_{min} in (a) and (b) and the ZPE in (c) give the solid curves in (a) and (b). ΔE^R, ΔE^P, and $\Delta E^‡$ denote the reactant, product, and transition state solvent coordinate values, respectively.

minimum switches between such positions at the TS, as shown in Figure 5, where for later reference the square ionic VB state coefficient at the minumum is shown as well. Figure 5a shows that there are two energetically degenerate proton potential minima at $\Delta E = 0$, which identifies the cause and location of the q_{min} switch.

As noted above, the ZPE displayed in Figure 4c reflects the change in the proton potential as a function of the solvent coordinate ΔE (Figure 1). The electronic adiabatic ground-state energy as a function of q gives the proton potential for a given ΔE. The modulation of the electronic structure—generally involving a mixture of both diabatic states—by the solvent, which differentially solvates the electronic diabatic neutral reactant and ionic product states, shifts this proton potential from favoring the donor-bound proton (Figure 1a) to favoring the acceptor-bound proton (Figure 1c). Of course at any ΔE value, the solute electronic structure varies with q, illustrated in Figure 5c showing the ionic VB state population c_I^2 for the symmetric reaction TS location $\Delta E = 0$, for which the proton potential is symmetric (Figure 1b). We emphasize that it is the ZPE that carries the major information on the smooth electronically adiabatic variation of the electronic structure through the proton potential barrier region seen in Figure 1. As will be shown in section 5, the *proton-averaged* solute electronic structure in the TS has equal contributions from both the neutral and ionic electronic VB states. The proton quantum average of c_I^2 is displayed in Figure 5b (solid line) and reflects the fact that the proton nuclear wave function associated with the ground

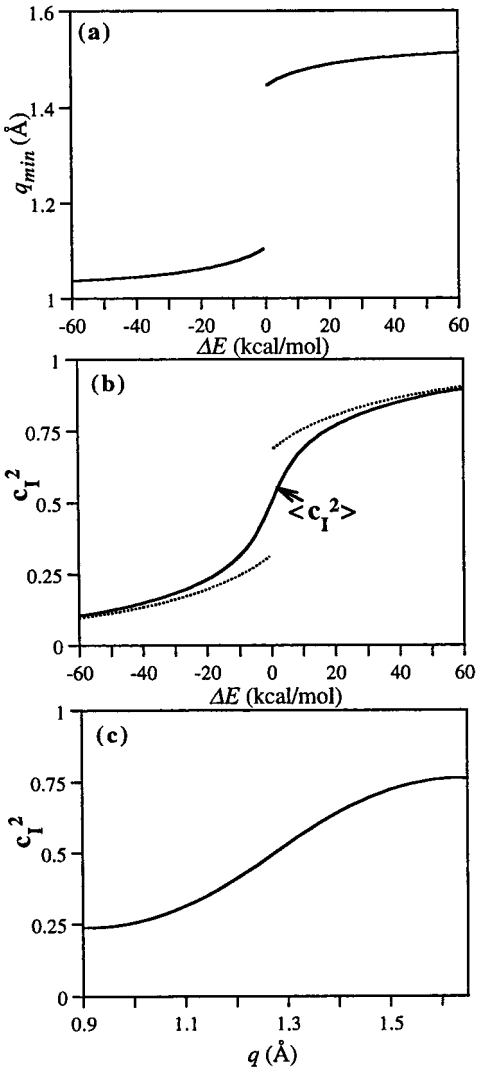

Figure 5. (a) Minimum location of the proton coordinate q_{min} versus ΔE for $Q = 2.55$ Å. (b) The square coefficient c_I^2 for the ionic VB state versus ΔE with $q = q_{min}$ (dashed line) and quantum averaged over the proton vibration (solid line). (c) The ionic electronic VB state square coefficient c_I^2, eq 2.11, versus the proton coordinate q for the symmetric reaction transition state value of the solvent coordinate $\Delta E = 0$.

vibrational state for the symmetric proton potential in Figure 1b has some delocalization between the donor and acceptor. At this point ($\Delta E = 0$), the ZPE has its minimum value due to the proton potential's symmetric double well character, and it exhibits a cusp, with the ZPE increasing going away from $\Delta E = 0$ as the solute structure and proton potential is dominated by either the neutral or ionic state and the proton moves accordingly in more confining R or P region potential wells. By contrast, G_{min} involves proton locations which remain largely *outside* this central barrier region, so that the associated electronic structure variation in each separate branch is fairly muted, though not negligible (cf. Figure 5b, dotted line).

An important feature of the ZPE in Figure 4c is that it applies for both the symmetric and the asymmetric cases Figure 4a and 4b; i.e., the ZPE is the *same* function of ΔE independent of ΔG_{RXN}. This property arises from the fact that changing ΔG_{RXN} does not change the proton potential's shape for a fixed ΔE. A change in ΔG_{RXN} does, however, shift the reference free energy at its minimum, G_{min}. Accordingly, the PT reaction thermodynamics or reaction asymmetry in Figure 4a and 4b will be dominated by G_{min}.

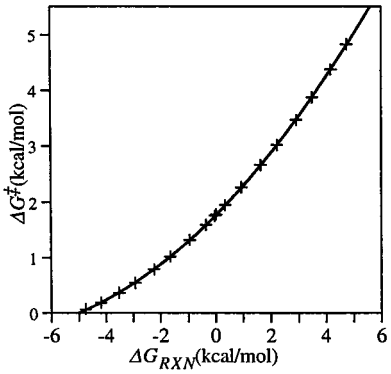

Figure 6. Free energy relationship $\Delta G^{\ddagger}$ vs. ΔG_{RXN} for fixed $Q = 2.55$ Å for a series of proton-transfer asymmetries (+). The solid line indicates a second-order numerical fit to the points. Points were generated from several free energy surfaces with different values of Δ_{vac}, as discussed in section 3.

The activation free energy $\Delta G^{\ddagger}$ versus reaction free energy ΔG_{RXN} profile for PT is plotted in Figure 6. The reaction barrier increases nonlinearly as the reaction goes from exothermic to endothermic, and in particular, the line displayed in Figure 6—a second-order fit to the calculated points—shows that a second-order free energy relationship is an excellent characterization in the current description, a key result analyzed further in section 5. The displayed range of ΔG_{RXN} in Figure 6 represents the relevant range for which an activation barrier exists, and thus defines the range in which a reaction rate constant can be defined.[53]

The R, P, and TS locations in Figure 4a and 4b are consistent with the Hammond postulate:[54,55] for an exothermic reaction, the TS is closer to the reactant (Figure 4b), and for an endothermic reaction, closer to the product (reverse of Figure 4b). Thus, the barrier in ΔE for PT decreases going from endothermic to exothermic, whereas the TS goes from being closer to the P to closer to the R. For a symmetric reaction (see Figure 4a and 4c), the proton ZPE, as well as G_{min}, is symmetric about $\Delta E = 0$, and thus G has this symmetry. When the reaction asymmetry changes, however, as previously discussed, G_{min} is no longer symmetric about $\Delta E = 0$, and the TS shifts toward the well which varies *least* near $\Delta E = 0$, toward R for exothermic reactions and toward P for endothermic reactions. Consequently, and this is an important point, the shift in the TS location to being more R- or P-like results from the *quantization* of the proton, i.e., the addition of ZPE to G_{min}. How the relative positions of the R, P, and transition states shift with respect to reaction asymmetry is related to the Brønsted coefficient, now discussed.

4b. Brønsted Coefficient. The first derivative of free energy with respect to reaction free energy is the Brønsted coefficient

$$\alpha = \partial \Delta G^{\ddagger} / \partial \Delta G_{RXN} \tag{4.1}$$

and has played a significant role in organic chemistry and biochemistry in characterizing various chemical reaction transition states.[55,4] For "normal" PT reactions, the Brønsted coefficient α lies between 0 and 1, and is usually interpreted as a measure of how similar the TS is to the product state (the larger, the more similar).[2,4,55,56] The explicit connection of α to the TS location will now be derived.

To begin, we recall that the variation of the reaction free energy ΔG_{RXN} in Figure 6 is achieved by varying the vacuum offset or asymmetry Δ_{vac} between the reactant and the product electronic diabatic states. Because both ΔG_{RXN} and the activation

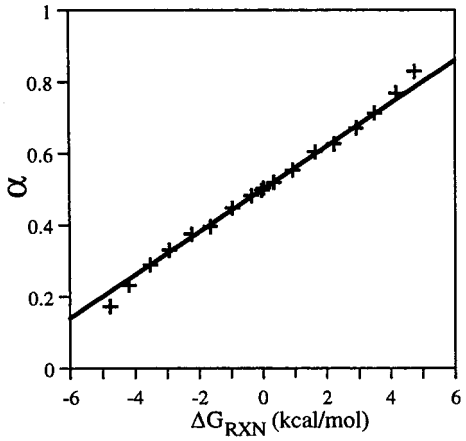

Figure 7. Plot of the Brønsted coefficient $\alpha = \partial\Delta G^{\ddagger}/\partial\Delta G_{RXN}$ versus the reaction free energy. Displayed are the numerical interpolations from the free energy curve in Figure 6 (line) and the calculated analytical expression eq 4.4 (+).

free energy $\Delta G^{\ddagger}$ vary with reaction asymmetry, a simple view of the Brønsted coefficient can be written as follows

$$\alpha = \partial\Delta G^{\ddagger}/\partial\Delta G_{RXN} = \partial\Delta G^{\ddagger}/\partial\Delta_{vac}/\partial\Delta G_{RXN}/\partial\Delta_{vac} \quad (4.2)$$

Both the free energy differences $\Delta G_{RXN} = G(\Delta E^P) - G(\Delta E^R)$ and $\Delta G^{\ddagger} = G(\Delta E^{\ddagger}) - G(\Delta E^R)$ are expressed as a difference in free energy between the appropriate critical points on the free energy curve (Figure 4). To proceed, we step back to the level of the free energy G_q before proton quantization was effected, i.e., eq 2.10. The partial derivative of this with respect to Δ_{vac} is given by

$$\frac{\partial G_q(q,Q,\Delta E)}{\partial\Delta_{vac}} = c_I^{\,2} \quad (4.3)$$

To incorporate proton quantization, c_I^2 is averaged over the ground-state proton vibrational wave function to give the expectation value $\langle c_I^2\rangle$ at a given ΔE. (Recall that the ZPE dependence on ΔE does not change as the reaction asymmetry is changed, and thus, quantization of the proton is dependent on ΔE but not on reaction asymmetry Δ_{vac}.) Evaluation in this fashion of the quantum average of c_I^2 at the R, P, and TS solvent configurations then gives the simple relation

$$\alpha = \partial\Delta G^{\ddagger}/\partial\Delta G_{RXN} = \frac{\langle c_I^2\rangle^{\ddagger} - \langle c_I^2\rangle^{R}}{\langle c_I^2\rangle^{P} - \langle c_I^2\rangle^{R}} \quad (4.4)$$

which is the fractional change of the (proton vibration-averaged) ionic character on going to the TS; α increases from 0 to 1 as the TS goes from being similar to R to being similar to P. Figure 7 is an overlay of the calculated ratio in eq 4.4 (points) with the Brønsted coefficient calculated from direct numerical evaluation of the slope (second-order fit to points) in Figure 6 versus ΔG_{RXN} (line); the excellent agreement supports the validity of the approximate eq 4.4 connecting α to the TS electronic structure, consistent with the Hammond postulate. (We postpone the explicit connection to the TS location in the solvent coordinate until section 5c.) α equals 0.5 for $\Delta G_{RXN} = 0$, such that the proton-averaged electronic structure at the TS is halfway between R and P for the symmetric reaction. Its variation away from that condition for finite ΔG_{RXN} is consistent with some,[37] but not all,[56a] treatments of other charge-transfer reactions.

5. Analytic Nonlinear Free Energy Relations

It has already been seen from Figures 6 and 7 that a second order $\Delta G^{\ddagger} - \Delta G_{RXN}$ relation is an accurate numerical characterization for PT in the present description. In this section, we derive an analytical form for the quadratic $\Delta G^{\ddagger}$ vs ΔG_{RXN} free energy relation for PT, based on the fundamental decomposition in eq 2.14 of the system free energy G into the two components G_{min} and ZPE. This derivation also allows the identification of coefficients, e.g., $\Delta G_o^{\ddagger}$, in terms of the underlying fundamental reaction features.

A second-order free energy relationship has three terms, the zero-order term being the "intrinsic" reaction barrier. The coefficient for the first-order term is α_o, the activation free energy derivative with respect to the reaction free energy, the Brønsted coefficient α, eq 4.1, evaluated for the symmetric reaction. The second-order coefficient α_o' is the derivative of α with respect to reaction asymmetry, evaluated for the symmetric reaction. Thus

$$\Delta G^{\ddagger} = \Delta G_o^{\ddagger} + \alpha_o\Delta G_{RXN} + \alpha_o'\frac{(\Delta G_{RXN})^2}{2} \quad (5.1)$$

In the following developments, to analyze eq 5.1, we begin with an analysis of G_{min} followed by that of the ZPE. These are then combined to deal with $\Delta G^{\ddagger}$, with the final major analytic result for $\Delta G^{\ddagger}$ obtained at eq 5.46.

5a. G_{min}. In this subsection, we first discuss the general features of G_{min}, its behavior with changing reaction asymmetry, and finally its barrier height for the reference symmetric reaction.

5a.1. Overview. As discussed in section 4.a, G_{min} is the system free energy with the proton fixed at its classical position q_{min} at the proton potential minimum, whose values in the R and P regions correspond to the equilibrium solvation energies of the fixed proton R and P solute structures. The condition defining q_{min} is, from eq 2.10

$$\frac{\partial Gq}{\partial q} = 0 = -(c_N^2F_{N,q} + c_I^2F_{I,q})\ (q = q_{min}) \quad (5.2)$$

involving the state average force on the proton, with e.g., $F_{N,q} = -\partial U_N/\partial q$. As discussed in section 4a, the cusp at $\Delta E = 0$ in G_{min} (see Figure 4) is a result of the switch between proton minimum positions q_{min} from being closer to the donor to being closer to the acceptor (Figure 5a). (Note carefully that this condition locates the equality of the free energies of the minima of the two wells in an electronically *adiabatic* double-welled proton potential.)

Figure 4 indicates the very important feature that G_{min} is evidently quite close to being double parabolic in nature, with a systematic shifting of the approximate parabolas as the reaction asymmetry changes. Certainly, neither this nearly parabolic character or its systematic shifting of G_{min} is immediately obvious from its formal definition, which from eq 2.10 is

$$G_{min}(q_{min};\Delta E) = \frac{1}{2K(\mu_N - \mu_I)^2}(\Delta G_d + \Delta E)^2 - \frac{K}{2}\left(\frac{\mu_N + \mu_I}{2}\right)^2 - \frac{K_\infty}{2}\left(\frac{\mu_N^2 + \mu_I^2}{2}\right) + \frac{\Delta_{vac}}{2} + \frac{U_N(q_{min}) + U_I(q_{min})}{2} - \frac{1}{2}\sqrt{(U_N(q_{min}) - U_I(q_{min}) + \Delta E)^2 + 4\beta^2} \quad (5.3)$$

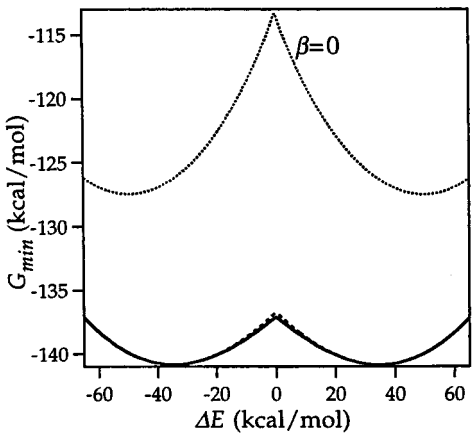

Figure 8. Comparison of G_{min} with (solid line) and without electronic coupling (dotted line) for a symmetric reaction ($\Delta G_d = 0$ kcal/mol, $\Delta_{vac} = 99.5$ kcal/mol). Also shown is G_{min} calculated with q_{min} held constant (dashed line); $q_{min} = 1.03$ Å for $\Delta E < 0$, and $q_{min} = 2.55 - 1.03 = 1.52$ Å for $\Delta E > 0$.

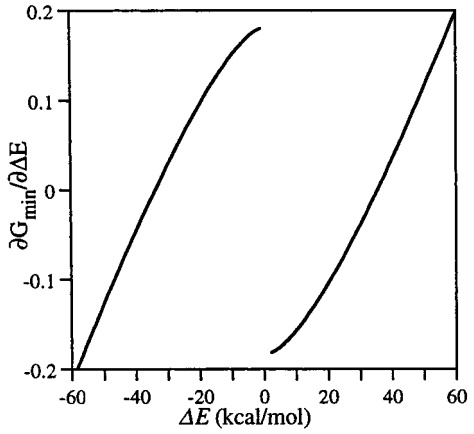

Figure 9. Derivative of G_{min} with respect to ΔE versus ΔE, for a symmetric reaction ($\Delta G_d = 0$ kcal/mol, $\Delta_{vac} = 99.5$ kcal/mol), showing that the double parabolic description of G_{min} has some deterioration near $\Delta E = 0$, as discussed in the text.

where the electron diabatic potentials U_N and U_I are evaluated at $q = q_{min}$. The first and last two terms in eq 5.3 carry the ΔE dependence (recall that q_{min} depends on ΔE). The first term is quadratic, whereas the last two terms are not, switching the ΔE location of the minimum of G_{min} from less than zero in the R region to greater than zero in the P region. If we momentarily consider for comparison the absence of significant electronic coupling $\beta \approx 0$, the second to last term is constant and the last term is linear in ΔE with a positive slope in the R region and a negative one in the P region. G_{min} would thus be exactly parabolic, as in the Marcus picture for weakly coupled ET reactions.[11] The PT reaction of interest here is, however, in the electronically *adiabatic* regime, with strong electronic coupling, and the significant electronic coupling present in eq 5.3 is the main reason for nonparabolic behavior in G_{min}, especially near $\Delta E = 0$. We hasten to stress that the electronic coupling is important over the *entire* ΔE range of relevance for G_{min}, as is illustrated in Figure 8, which compares G_{min} to the value G_{min}^{diab} evaluated at zero electronic coupling $\beta = 0$. Even in the R and P wells, the electronic coupling mixes the neutral and ionic VB states to a significant degree, and at no point is it legitimate to adopt a nonadiabatic perspective. Our remarks above emphasize that the electronic coupling is always important, but it is *more* important near $\Delta E = 0$.

In what follows, we will require both the first and second derivatives of G_{min} with respect to ΔE. From eq 5.3, the first of these is

$$\frac{\partial G_{min}}{\partial \Delta E} = \frac{1}{K(\mu_N - \mu_I)^2}(\Delta G_d + \Delta E) - \frac{\partial q_{min}}{\partial \Delta E}\left(\frac{F_{N,q_{min}} + F_{I,q_{min}}}{2}\right) + \left(\frac{1}{2} - c_I^2(q_{min};\Delta E)\right)\left(1 - \frac{\partial q_{min}}{\partial \Delta E}(F_{N,q_{min}} - F_{I,q_{min}})\right) = \frac{1}{K(\mu_N - \mu_I)^2}(\Delta G_d + \Delta E) + \left(\frac{1}{2} - c_I^2(q_{min};\Delta E)\right) \quad (5.4)$$

where we have used the q_{min} condition eq 5.2 to arrive at the second form; this is plotted in Figure 9 for later reference. From eq 5.4, the second derivative of G_{min} is

$$\frac{\partial^2 G_{min}}{\partial \Delta E^2} = \frac{1}{K(\mu_N - \mu_I)^2} - \frac{\partial c_I^2(q_{min}, \Delta E)}{\partial \Delta E} \quad (5.5)$$

It should be noted that unlike the first derivative of G_{min}, eq 5.4, the second derivative is independent of reaction asymmetry, i.e., independent of ΔG_d.

The positions of the critical points of G_{min} are easily found with eq 5.4. The maximum of G_{min} is always located exactly at $\Delta E = 0$, independent of reaction asymmetry ($\Delta E_m^{\ddagger} = 0$, see Figure 4); the classical proton position q_{min} always switches from R to P at $\Delta E = 0$. The ΔE positions of the R and P minima can be found by setting the first derivative in eq 5.4 to zero

$$\Delta E_m = -K(\mu_N - \mu_I)^2\left(\frac{1}{2} - c_I^2(q_{min};\Delta E_m)\right) - \Delta G_d \quad (5.6)$$

The vertical displacement in free energy of these minima defines a reaction asymmetry associated with G_{min}

$$\Delta_m = G_{min}(\Delta E_m^P) - G_{min}(\Delta E_m{}^R) \quad (5.7)$$

As a final item in these preliminaries, evaluation of eq 5.5 at e.g., ΔE_m^R

$$k_m = \frac{1}{K(\mu_N - \mu_I)^2} - \left.\frac{\partial c_I^2(q_{min},\Delta E)}{\partial \Delta E}\right|_{\Delta E_m{}^R} \quad (5.8)$$

defines a harmonic force constant k_m for G_{min}; the first term is the electronically diabatic force constant

$$k_d = 1/K(\mu_N - \mu_I)^2 \quad (5.9)$$

modified in k_m by the second term, involving the electronic structure variation. Due to the intrinsically symmetric nature of the two valence bond potentials, k_m is the same for both the R and P wells.[42] Figure 9 indicates that the harmonic approximation with the G_{min} force constant defined in the R well, eq 5.8, will deviate near the cusp. The dashed line in Figure 8 shows that the stretching of the proton, going from its R minimum value to its value at the cusp $\Delta E = 0$—which one might suspect to be responsible—is only a minor contribution; in section 5a.3, we show the deviation is largely due to the influence of an electronic structure change.

5a.2. Asymmetry Variation of G_{min}. We now characterize the asymmetry variation of the barrier height

$$\Delta G^{\ddagger}_{m} = G_{min}(\Delta E = 0) - G_{min}(\Delta E_m{}^R) \qquad (5.10)$$

in terms of its value $\Delta G^{\ddagger}_{m,o}$, for the symmetric reaction and the asymmetry Δ_m, eq 5.7. Because the peak of G_{min} occurs at $\Delta E = 0$ no matter what Δ_m is, this will entail the investigation of $G_{min}(\Delta E_m{}^R)$'s behavior with Δ_m.

For this purpose, it will prove convenient to begin by expanding G_{min} through second order in ΔE about the equilibrium positions, $\Delta E^{R,P}_{m,o} = \mp\Delta E_o$, for the symmetric reaction which as will be seen, is guaranteed by the condition $\Delta G_d = 0$

$$G^{R,P}_{min} = G^{R,P}_{m,o} + \frac{k_d}{2}[(\Delta G_d + \Delta E)^2 - (\Delta E_o)^2] \pm A(\Delta E \pm \Delta E_o) - \frac{B}{2}(\Delta E \pm \Delta E_o)^2 \qquad (5.11)$$

in which $G_{m,o}{}^{R,P}$ are the values of G_{min} for the respective equilibrium positions, and A and B are defined by the first and second derivatives

$$\pm A = \left(\frac{1}{2} - c_I^2(q_{min};\Delta E)\right)|_{\mp\Delta E_o};\ B = \frac{\partial c_I^2(q_{min};\Delta E)}{\partial \Delta E}|_{\mp\Delta E_o} \qquad (5.12)$$

involving the electronic structure. A and B are identical in the R and P regions due to the symmetric nature of the electronically diabatic states (e.g., $V_I(q)$=$V_N(Q-q)$).[42]

The first derivative of G_{min} evaluated for $\Delta G_d = 0$ identifies ΔE_o as

$$\Delta E_o = A/k_d \qquad (5.13)$$

consistent with eq 5.6, and identifies the G_{min} R and P minima locations for the general asymmetric case ($\Delta G_d \neq 0$) as

$$\Delta E^{R,P}_m = \mp\Delta E_o - \frac{k_d}{k_m}\Delta G_d \qquad (5.14)$$

where $k_m = k_d - B$ is the harmonic force constant for G_{min} defined in eq 5.8, a result consistent with the expansion of eq 5.6. The distance between these minima

$$\Delta\Delta E_m = \Delta E^P_m - \Delta E_m{}^R = 2\Delta E_o \qquad (5.15)$$

is independent of the reaction asymmetry.

Insertion of eq 5.14 into eq 5.11 gives

$$G^{R,P}_{min} = G^{R,P}_{m,o} + \frac{k_d}{2}\left(1 - \frac{k_d}{k_m}\right)\Delta G_d{}^2 \mp k_d\Delta E_o\Delta G_d \qquad (5.16)$$

so that the reaction asymmetry eq 5.7 is

$$\Delta_m = 2k_d\Delta E_o\Delta G_d \qquad (5.17)$$

indicating that the reaction asymmetry for G_{min} scales linearly with ΔG_d and, as stated above eq 5.11, $\Delta G_d = 0$ defines a symmetric reaction.

Finally, the forward and reverse barrier heights are, from eqs 5.16 and 5.17

$$\Delta G^{\ddagger}_{m,f,r} = G^{\ddagger}_m - G^{R,P}_m = \Delta G^{\ddagger}_{m,o} + \frac{1}{2}k_d\Delta G_d^2 - G^{R,P}_m = \Delta G^{\ddagger}_{m,o} \pm \frac{\Delta_m}{2} + \frac{1}{2k_m\Delta\Delta E_m^2}\Delta_m^2 \qquad (5.18)$$

related appropriately by $\Delta G^{\ddagger}_{m,f} = \Delta G^{\ddagger}_{m,r} + \Delta_m$.

5a.3. Intrinsic Barrier for G_{min}. It remains to characterize $\Delta G^{\ddagger}_{m,o}$ in eq 5.18, the barrier height associated with G_{min} in the symmetric case $\Delta_m = 0$. This turns out to be the most difficult aspect of the entire treatment, and although we are not able to derive a simple analytical expression for $\Delta G^{\ddagger}_{m,o}$ that is very highly accurate, we will be able to find an expression that, while not complex, gives a reasonably numerically accurate description while including the key features of $\Delta G^{\ddagger}_{m,o}$.

A first approach, motivated by the near double parabolic form exhibited by G_{min} in Figure 4 would be to use a simple parabolic form for the derivation of the free energy relationship

$$G_{min} = \frac{1}{2}k_m(\Delta E - \Delta E^R_m)^2;\ \Delta E < 0 = \Delta_m + \frac{1}{2}k_m(\Delta E - \Delta E^P_m)^2;\ \Delta E > 0 \qquad (5.19)$$

where k_m is the harmonic force constant eq 5.8. Then $\Delta G^{\ddagger}_{m,o}$ would equal $\lambda_m = 1/2k_m(\Delta E^R_{m,o})^2$, which one could use to define a reorganization energy

$$\lambda_m = \frac{1}{2}k_m(\Delta E^P_m - \Delta E_m{}^R)^2 \qquad (5.20)$$

such that the intrinsic barrier would be

$$\Delta G^{\ddagger}_{m,o} \approx \frac{\lambda_m}{4} \qquad (5.21)$$

This definition, although it captures signficant aspects of the G_{min} barrier height, is an overestimate by about 20% ($\Delta G^{\ddagger}_{m,o}$ = 3.75 kcal/mol, whereas eq 5.21 gives 4.43 kcal/mol). This shortcoming arises from the important feature that in a strongly electronically adiabatic PT reaction, the electronic structure, e.g., c_I^2, shifts between the minimum location ΔE^R_o and the barrier location $\Delta E = 0$, as exemplified by the curvature of the first derivative of G_{min} near $\Delta E = 0$ displayed in Figure 9 (Note that the 'local' force constant, the second derivative eq 5.5, will vary between the two points.) We show in Appendix A that a partial accounting of this anharmonic variation improves upon eq 5.21 somewhat, giving

$$\Delta G^{\ddagger}_{m,o} = \frac{\lambda_m}{4} - \frac{1}{6}\Delta E_o{}^3\frac{\partial 2c_I^2}{\partial \Delta E^2}|_{-\Delta E_o} = \frac{\lambda_m}{4} - \Delta E_o{}^3\frac{c_I^4\, c_N^4}{\beta^2}(c_N^2 - c_I^2)|_{-\Delta E_o} \qquad (5.22)$$

This approximation reduces the overestimate to only 5% (eq 5.22 gives $\Delta G^{\ddagger}_{m,o}$ = 3.85 kcal/mol compared to the correct value 3.75 kcal/mol), which would be satisfactory for most purposes.[57] In effect, it is as if the reorganization energy λ_m is reduced, because the solvent is in the presence of a solute charge

distribution which is not fixed on going from R to TS, as seen in Figure 5b (dotted line).

In concluding this subsection, we should emphasize the meaning of any reorganization energy in connection with $\Delta G^{\ddagger}_{m,o}$. The reorganization involved is essentially that of the solvent. Figure 8 shows the important point that the reorganization energy is considerably less than would be predicted from any electronically diabatic view (as in outer sphere ET). This reduction has two basic sources. The first is that even in the R well, the solute pair already has a mixed electronic structure (finite c_I^2), and the second is—as just discussed—that this electronic structure continues to evolve with ΔE; at the cusp $\Delta E = 0$, the solvent is in the presence of a reactant pair with an even higher ionic character than in the reactant (Figure 5b).[58]

5b. Zero Point Energy (ZPE). The nonlinearity of the Schrodinger eq 2.13 prevents a closed form analytical expression for the ZPE, but it can be described by expanding through second order around the three critical points for the R, P, and TS regions. In particular, it is convenient to expand the ZPE, as in eq 5.11, around the critical points of G_{min} for a symmetric reaction ($\Delta E^{\ddagger} = 0$, $\Delta E_m{}^R = -\Delta E_o$, $\Delta E_m{}^P = \Delta E_o$); note that these are not the critical points for either G_{min} in general or G. In the R and P regions, the ZPE is given by

$$ZPE(\Delta E) = Z^{R,P}_{m,o} \mp a(\Delta E \pm \Delta E_o) - \frac{1}{2}b(\Delta E \pm \Delta E_o)^2 \quad (5.23)$$

where $Z^{R,P}_{m,o} = ZPE(\mp\Delta E_o)$ and the coefficients a and b describe the first and second ZPE derivatives at $\Delta E = \mp\Delta E_o$. In the TS region $\Delta E \approx 0$, the ZPE is given by

$$ZPE(\Delta E) = Z^{\ddagger}_{m,o} \mp a^{\ddagger}\Delta E - \frac{1}{2}b^{\ddagger}\Delta E^2 \quad (5.24)$$

where $Z^{\ddagger}_{m,o}$ and the coefficients $\mp a^{\ddagger}$ and $-b^{\ddagger}$ are the first and second ZPE derivatives at $\Delta E = 0$. The sign of the first-order term in eqs 5.23 and 5.24 reflects the equal but opposite slope in the R and P regions.[42] Both ZPE and G_{min} are discontinuous at $\Delta E = 0$, but the sum gives a continuous full free energy G. The condition $b^{\ddagger} > k_m$ for the free energy guarantees a maximum.

The coefficients in the above expansions related to the derivatives of the ZPE will now be shown to be related to the difference between the electronic structure with the proton quantized versus the proton classical. As a preliminary to this demonstration, we need to return to eq 2.14 for the free energy G_q prior to proton quantization. On taking its derivative with respect to the reaction coordinate ΔE and averaging over the ground-state proton vibrational wave function for each value of ΔE, one has

$$\frac{\partial G}{\partial \Delta E} = k_d(\Delta G_d + \Delta E) + \frac{1}{2} - \langle c_I{}^2(\Delta E)\rangle \quad (5.25)$$

involving the expectation value $\langle c_I^2\rangle$.

With the use of eqs 2.14, 5.4, and 5.25, the first derivative is given by

$$\frac{\partial ZPE(\Delta E)}{\partial \Delta E} = \frac{\partial G(\Delta E)}{\partial \Delta E} - \frac{\partial G_{min}(\Delta E)}{\partial \Delta E}$$

$$= -\langle c_I{}^2(\Delta E)\rangle + c_I^2(q_{min};\Delta E) \quad (5.26)$$

and the second derivative is

$$\frac{\partial ZPE(\Delta E)}{\partial \Delta E} = -\frac{\partial}{\partial \Delta E}(\langle c_I^2(\Delta E)\rangle - c_I^2(q_{min};\Delta E)) \quad (5.27)$$

The first and second-order coefficients in the expansions 5.23 and 5.24 are thus given by eqs 5.26 and 5.27.

5c. PT System Free Energy *G*. The desired full free energy G is found by addition of the ZPE to G_{min}. In the R and P regions, G is the sum of eqs 5.11 and 5.23. The positions of G's critical points are easily found as

$$\Delta E^{R,P} = \mp\left(\Delta E_o - \frac{a}{k_R}\right) - \frac{k_d\Delta G_d}{k_R} \quad (5.28)$$

where $k_R = k_d - B - b = k_m - b$ is the force constant for G for R (and P). This is the explicit implementation of the formal result for the critical points ΔE_c of G

$$\Delta E_c = -K(\mu_N - \mu_I)^2\left(\frac{1}{2} - \langle c_I^2(\Delta E_c)\rangle\right) - \Delta G_d \quad (5.29)$$

which follows from eq 5.25, and comparison of eqs 5.29 and 5.25 with eqs 5.4 and 5.6 shows that the minima of G and G_{min} are shifted due to the difference in the proton quantum average of c_I^2 and its value at the classical proton postion.

With eq 5.28, the free energies at the R and P minima are

$$G^{R,P} = G^{R,P}_{m,o} + Z^{R,P}_{m,o} + \frac{1}{2}k_d(\Delta G_d \mp \Delta E_o)^2 - \frac{1}{2}k_d\Delta E_o{}^2 - \frac{1}{2}\frac{(k_d\Delta G_d \mp a)^2}{k_R} \quad (5.30)$$

The PT reaction asymmetry is

$$\Delta G_{RXN} = G^P - G^R = \Delta_m\left(1 - \frac{a}{k_R\Delta E_o}\right) \quad (5.31)$$

which shows explicitly that ΔG_{RXN} is not just the asymmetry Δ_m of G_{min}: the shifts of the minima of G from those of G_{min} occur in both the R and P regions due to the ZPE and lead to the second term in eq 5.31.

In the TS region, G is the sum of the ZPE expansion in eq. 5.24 and an expansion of G_{min} around $\Delta E = 0$

$$G^{\ddagger}_{min} = G^{\ddagger}_{m,o} + \frac{k_d}{2}(\Delta G_d + \Delta E)^2 \pm A^{\ddagger}\Delta E - \frac{B^{\ddagger}}{2}\Delta E^2 \quad (5.32)$$

where $A^{\ddagger}$ and $B^{\ddagger}$ are the first and second derivatives of G_{min}, respectively, evaluated at $\Delta E = 0$ (see eqs 5.4 and 5.5), where the relationship $A^{\ddagger} = a^{\ddagger}$ ensures that G is continuous. The TS position is

$$\Delta E^{\ddagger} = \frac{k_d\Delta G_d}{k^{\ddagger}} = \frac{\Delta_m}{2k^{\ddagger}\Delta E_o} \quad (5.33)$$

where $k^{\ddagger} = B^{\ddagger} + b^{\ddagger} - k_d$ is the magnitude of the unstable force constant for G at the TS. Comparison of this with eq 5.29 shows that for the symmetric reaction, $\Delta G_{RXN} \propto \Delta_m \propto \Delta G_d = 0$, the proton-averaged electronic structure at the TS is an equal mixture of the neutral and ionic structures, $\langle c_N^2\rangle = \langle c_I^2\rangle = 0.5$, with a corresponding shift of the proton-averaged electronic

structure in the asymmetric case, depending on ΔG_{RXN}. The free energy at the TS is thus

$$G^{\ddagger} = G^{\ddagger}_{m,o} + Z^{\ddagger}_{m,o} + \frac{1}{2}\frac{{\Delta_m}^2}{\Delta\Delta E_m{}^2}\left(\frac{1}{k_d} + \frac{1}{k^{\ddagger}}\right) \qquad (5.34)$$

With these results, we have the full PT reaction barrier given by

$$\Delta G^{\ddagger} = G^{\ddagger} - G^{R}$$
$$= G^{\ddagger}_{m,o} + Z^{\ddagger}_{m,o} - Z^{R}_{m,o} + \frac{1}{2}\frac{a^2}{k_R} + \frac{\Delta_m}{2}\left(1 - \frac{2a}{k_R\Delta\Delta E_m}\right) + \frac{1}{2}\frac{\Delta_m^2}{\Delta\Delta E_m^2}\left(\frac{1}{k^{\ddagger}} + \frac{1}{k_R}\right) \qquad (5.35)$$

and eqs 5.31 and 5.35 give the desired second-order free energy relation as

$$\Delta G^{\ddagger} = G^{\ddagger}_{m,o} + Z^{\ddagger}_{m,o} - Z^{R}_{m,o} + \frac{1}{2}\frac{a^2}{k_R} + \frac{\Delta G_{RXN}}{2} + \frac{1}{2}\frac{\Delta G^2_{RXN}}{\Delta\Delta E_m^2}\left(\frac{1}{k^{\ddagger}} + \frac{1}{k_R}\right)\Big/\left(1 - \frac{2a}{k_R\Delta\Delta E_m}\right)^2 \qquad (5.36)$$

The interpretation, and some reformulation, of the three contributions to this free energy relation corresponding to the different powers of ΔG_{RXN} will now be discussed in turn.

5c.1. Intrinsic Reaction Barrier. The PT free energy barrier's first component is the intrinsic barrier $\Delta G^{\ddagger}_o$ for a symmetric PT reaction (cf. Figure 4a); from eq 5.36, this is

$$\Delta G^{\ddagger}_o = \Delta G^{\ddagger}_{m,o} + \Delta Z^{\ddagger}_{m,o} - Z^{R}_{m,o} + \frac{1}{2}\frac{a^2}{k_R} \qquad (5.37)$$

which we now discuss and reformulate.

The addition of the ZPE to G_{min} has shifted the position of the R minimum for G from the minimum ΔE^R_m in G_{min} closer to $\Delta E = 0$ (Figure 4a), with consequent shifts in energy for both G_{min} and ZPE in the R region. The last term in eq 5.37 contains these energy shifts, and in particular, contains the difference between the ZPE evaluated at the R location for G_{min}, $\Delta E = -\Delta E_o$ ($Z^R_{m,o}$) and the ZPE Z^R_o evaluated at the R location ΔE^R for G for a symmetric reaction. The other shift in energy included in the last term in eq 5.37 is that of G_{min} and is smaller than this. Because the magnitudes of these shifts are small relative to $Z^R_{m,o}$, the sum of last two terms is approximately the ZPE of the reactant state Z^R_o. Thus, the intrinsic free energy barrier is well approximated by the intrinsic barrier for G_{min} plus the difference in ZPE between the reactant and transition state for the symmetric reaction (note that $Z^{\ddagger}_o = Z^{\ddagger}_{m,o}$)

$$\Delta G^{\ddagger}_o = \Delta G^{\ddagger}_{m,o} + Z^{\ddagger}_o - Z_o{}^R \qquad (5.38)$$

with $\Delta G^{\ddagger}_{m,o}$ given by eq 5.22. The validity of this result can be established by comparison with Figure 6, which gives $\Delta G^{\ddagger}_o = 1.76$ kcal/mol, whereas eq 5.38 gives $\Delta G^{\ddagger}_o = 1.73$ kcal/mol.

Equation 5.38 explicitly expresses the physical perspective presented in section 4a, here specialized to the symmetric reaction case: the barrier for PT is determined by a barrier dominated by environmental reorganization and the change in the ZPE of the quantized proton. The effect of the latter is to reduce the intrinsic barrier compared to the former: the ZPE change in eq 5.38 is negative, reflecting the greater proton delocalization and lower ZPE at the TS compared to the reactant. This is definitely a nonnegligible effect: for the present model system, from Figure 4, $\Delta G^{\ddagger}_{m,o} = 3.76$ kcal/mol, whereas the ZPE change contribution is -2.0 kcal/mol. It is important to emphasize that any such effect would be absent in traditional approaches, since for a symmetric reaction, the transverse coordinate at the TS is considered independent of the proton coordinate,[1,4,19] and no proton ZPE contribution can arise. But in the present description, the transition state ZPE enters because the proton coordinate is *transverse* to the solvent reaction coordinate, and is not itself the reaction coordinate.

5c.2. Brønsted Coefficient and its Derivative for the Symmetric PT Reaction. From the general expansion eq 5.1, the terms linear and quadratic in ΔG_{RXN} in eq 5.36 are related to the Brønsted coefficent α, eqs 4.1 and 4.4. To proceed, it is useful to employ eq 5.29 to describe the electronic structure in terms of the critical point solvent coordinate positions, such that eq 4.4 for α now becomes

$$\alpha = \frac{\partial\Delta G^{\ddagger}}{\partial\Delta G_{RXN}} = \frac{\langle c_I^2\rangle^{\ddagger} - \langle c_I{}^2\rangle^R}{\langle c_I^2\rangle^P - \langle c_I{}^2\rangle^R} = \frac{\Delta E^{\ddagger} - \Delta E^R}{\Delta E^P - \Delta E^R} \qquad (5.39)$$

which incidentally provides further insight into the Brønsted coefficient itself. In particular, it quantifies the reaction coordinate analysis of the Hammond postulate, discussed qualitatively in section 4b: an endothermic (exothermic) reaction has a late (early) transition state. Equation 5.39 is an important expression for the present perspective: the quantum proton-averaged solute electronic structure is *directly correlated* with the differential solvation reaction coordinate. (See our remark at the very end of section 4).

The coefficients for the first and second-order terms in eq 5.1 are determined by α and its derivative evaluated for the symmetric reaction, $\Delta G_{RXN} = 0$. From eq 5.31, $\Delta G_{RXN} = 0$ occurs when $\Delta_m = 0$, giving $\Delta E^{\ddagger} = 0$ and $\Delta E^R = -\Delta E^P$. Substitution of these into eq 5.39 gives the first-order term, $\alpha_o = 1/2$. The second-order term is more complex, and we begin by noting that the derivative of eq 5.39 is

$$\alpha' = \frac{\partial}{\partial\Delta G_{RXN}}\left(\frac{\Delta E^{\ddagger} - \Delta E^R}{\Delta E^P - \Delta E^R}\right) \qquad (5.40)$$

The relative distance between the R and P minima is not expected to change significantly as the reaction asymmetry is changed, and indeed this follows from eq 5.28. Thus α' can be cast in the form

$$\alpha' \approx \frac{1}{\Delta E^P - \Delta E^R}\frac{\partial(\Delta E^{\ddagger} - \Delta E^R)}{\partial\Delta G_{RXN}} \qquad (5.41)$$

i.e., the relative change with respect to ΔG_{RXN} of the R to TS distance along the reaction coordinate, normalized by the distance between the R and P states.

The (numerically) linear Brønsted relationship displayed in Figure 7 suggests that eq 5.41 is essentially constant near $\Delta G_{RXN} = 0$, and thus suggests that the critical point positions change linearly with respect to reaction asymmetry, a behavior consistent with eqs 5.28 and 5.33, which give

$$\Delta E^{\ddagger} - \Delta E^R = \frac{1}{2}(\Delta E^P - \Delta E^R) + \frac{\Delta G_{RXN}}{\Delta E^P - \Delta E^R}\left(\frac{1}{k^{\ddagger}} + \frac{1}{k_R}\right) \qquad (5.42)$$

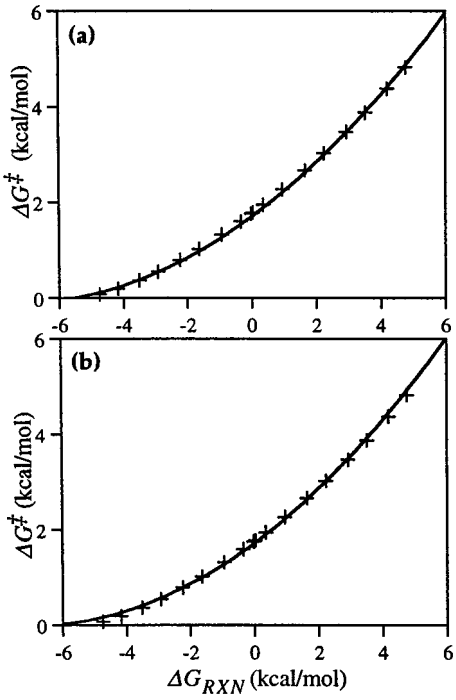

Figure 10. Free energy relationship $\Delta G^{\ddagger}$ vs. ΔG_{RXN} for fixed Q = 2.55 Å for a series of proton-transfer asymmetries (+). The solid line in (a) corresponds to eq 5.46 using $\Delta G_{\mathrm{o}}^{\ddagger} = 1.73$ kcal/mol and $\alpha_{\mathrm{o}}' = 0.056$ mol/kcal, and the solid line in (b) indicates a *numerical* fit of the data to eq 1.1 ($\Delta G_{\mathrm{o}}^{\ddagger}$ =1.72 kcal/mol).

Then α is

$$\alpha = \frac{1}{2} + \frac{\Delta G_{\mathrm{RXN}}}{(\Delta E^{P} - \Delta E^{R})^{2}}\left(\frac{1}{k^{\ddagger}} + \frac{1}{k_{\mathrm{R}}}\right) \qquad (5.43)$$

and its derivative is obviously

$$\alpha' = \alpha_{\mathrm{o}}' = \frac{1}{(\Delta E^{P} - \Delta E^{R})^{2}}\left(\frac{1}{k^{\ddagger}} + \frac{1}{k_{\mathrm{R}}}\right) \qquad (5.44)$$

which is exactly the same as the detailed second derivative of eq 5.36

$$\alpha' = \alpha_{\mathrm{o}}' = \frac{1}{\Delta\Delta E_{\mathrm{m}}^{2}}\left(1 - \frac{2a}{k_{\mathrm{R}}\Delta\Delta E_{\mathrm{m}}}\right)^{-2}\left(\frac{1}{k^{\ddagger}} + \frac{1}{k_{\mathrm{R}}}\right) \qquad (5.45)$$

We note for later reference that the ZPE curvature at the TS and R enters these results in a fundamental way, e.g., via the presence of the b terms in the force constants $k^{\ddagger}$ and k_{R}. The validity of eq 5.44 can be checked by noting that the observed Brønsted plot slope is 0.06 mol/kcal in Figure 7, whereas eq 5.44 gives 0.056 mol/kcal.

In summary, from the above analysis, the free energy relation governing the fixed proton donor−acceptor separation PT system is

$$\Delta G^{\ddagger} = \Delta G_{\mathrm{o}}^{\ddagger} + \alpha_{\mathrm{o}}\Delta G_{\mathrm{RXN}} + \frac{1}{2}\alpha_{\mathrm{o}}'\Delta G_{\mathrm{RXN}}^{2}$$

$$\approx \Delta G_{\mathrm{m,o}}^{\ddagger} + Z_{\mathrm{o}}^{\ddagger} - Z_{\mathrm{o}}^{R} + \frac{\Delta G_{\mathrm{RXN}}}{2} + \frac{1}{2}\alpha_{\mathrm{o}}'\Delta G_{\mathrm{RXN}}^{2} \qquad (5.46)$$

with $\Delta G_{\mathrm{m,o}}^{\ddagger}$ given to within 5% by eq 5.22 and with α'_{o} given explicitly by eq 5.44. This is the main explicit analytic result of the present paper, and the excellent agreement between eq 5.46 and the data in Figure 6 is shown in Figure 10a.

5d. Reaction Barrier Height versus Reaction Asymmetry and the Marcus Free Energy Relation. Our basic result eq 5.46 is clearly similar to the Marcus relation eq 1.1 in several aspects, e.g., $\alpha = 0.5$ when $\Delta G_{\mathrm{RXN}} = 0$ is common to both. There is however, the obvious difference that in our result eq. 5.46 (and 5.44), the coefficient of the term quadratic in ΔG_{RXN} differs from that ($1/16\Delta G_{\mathrm{o}}^{\ddagger}$) in the Marcus relation. From a fundamental point of view, e.g., eq 5.40, α_{o}' depends on how the relative distance between the reactant and transition states changes with reaction asymmetry in the neighborhood of $\Delta G_{\mathrm{RXN}} = 0$, and for adiabatic PT this explicitly depends on how the ZPE *varies* with ΔG_{RXN}. By contrast, the intrinsic barrier only depends on the *magnitude* of the ZPE change on going from the reactant to the symmetric transition state, and this has no contribution from the variation of ZPE in the neighborhood of $\Delta G_{\mathrm{RXN}} = 0$. This feature—which is reflected in the presence of the R and TS force constants involving the ZPE derivative in eq 5.44 for α_{o}', but not in eq 5.38 for the intrinsic barrier $\Delta G_{\mathrm{o}}^{\ddagger}$—indicates that α_{o}' should not be, and is not, solely expressible in terms of $\Delta G_{\mathrm{o}}^{\ddagger}$. On the other hand, the *numerical* consequences of this fundamental difference need not be at all severe, and indeed Figure 10b shows that using eq 1.1 to *fit* the free energy behavior does an excellent job of representing the PT free energy variation. The reasons for this somewhat accidental success can be assessed as follows. The ratio $\alpha_{\mathrm{o}}'/(1/8\Delta G_{\mathrm{o}}^{\ddagger})$ between the correct coefficient α_{o}', and its replacement ($1/8\Delta G_{\mathrm{o}}^{\ddagger}$) in eq 1.1 is close to unity for the model systems presented here, a numerical similarity which can be understood. We analyze eq 5.44 for α_{o}' in Appendix B to express it in the *empirical* form

$$\alpha_{\mathrm{o}}' = \frac{f}{8\Delta G_{\mathrm{o}}^{\ddagger}} \qquad (5.47)$$

so that our free energy relation eq 5.46, can be written as

$$\Delta G^{\ddagger} = \Delta G_{\mathrm{o}}^{\ddagger} + \frac{\Delta G_{\mathrm{RXN}}}{2} + \frac{f}{16\Delta G_{\mathrm{o}}^{\ddagger}}\Delta G_{\mathrm{RXN}}^{2} \qquad (5.48)$$

and will *numerically* match the Marcus relation eq 1.1 if $f \approx 1$. In appendix B, it is indicated that $f = 0.8$, which is indeed close to unity despite the strong conceptual distinctions between α_{o}' and $\Delta G_{\mathrm{o}}^{\ddagger}$ we have emphasized above.

It should also be pointed out that the importance of the quadratic term is somewhat muted by the feature that the limits of the free energy relationship are restricted by the requirement of a free energy barrier to define a rate. Qualitatively, the barrier height $\Delta G^{\ddagger}$ vanishes in our picture when the barrier height in G_{min} is canceled by the reactant−transition state ZPE difference. Quantitatively, the limits are defined by setting eq. 5.46 equal to zero, giving the limiting reaction asymmetries as

$$\Delta G_{\mathrm{RXN}} = \pm\frac{1}{2\alpha_{\mathrm{o}}'}[1 - \sqrt{1 - 8\alpha_{\mathrm{o}}'\Delta G_{\mathrm{o}}^{\ddagger}}] \qquad (5.49)$$

which are $\sim\pm5$ kcal/mol in Figure 6. In contrast to such relatively modest asymmetries, much larger values are possible for nonadiabatic tunneling PT reactions, which would thus provide a more sensitive probe of quadratic terms in free energy relations.

6. Concluding Remarks

In this paper, we have been able to find a nonlinear FER (eq 5.46) of the type widely successful in application to experimental

results in solution for proton transfer reaction rates versus reaction thermodynamics, based on a nonconventional quantum adiabatic picture for the proton transfer, in which the reaction coordinate and barrier involve the reorganization of the solvent, rather than the proton itself. The ingredients in this nonlinear FER have been analytically derived. In particular, the intrinsic free energy barrier $\Delta G_o^{\ddagger}$ was explicitly related to (eq 5.38) the reorganization of the solvent and the change of the zero point energy of the quantum proton between the reactant and the transition state configurations of the solvent coordinate. The nonlinear FER was found to differ numerically in only a minor fashion from the often-employed Marcus nonlinear free energy equation, where for the latter the intrinsic free energy barrier is simply regarded as a numerical parameter to be fit. It was shown that this numerical agreement is a reflection of the feature that often the range of thermodynamic reaction asymmetry is sufficiently restricted that the quadratic term in a nonlinear FER is not sensitively probed, such that the fundamentally different identifications of this term—related to the variation of the Bronsted coefficient with thermodynamic reaction asymmetry—in the present treatment and in the Marcus equation will not typically be apparent. Even in this circumstance, there remains the important feature that the intrinsic free energy barrier has been explicitly characterized in the present work.

The present treatment was restricted, for simplicity, to the situation where the H-bond coordinate—the distance between the proton donor and acceptor—is held fixed. This restriction is removed in the following paper, where it is shown that generally the same fundamental results follow, with some differences in interpretation, related to the important influence of the H-bond vibration.

Acknowledgment. This work was supported in part by NSF Grants CHE-9700419 and CHE-0108314. PK acknowledges the support of an NIH Postdoctoral Fellowship.

Appendix A: Intrinsic Reaction Barrier for G_{min}

To analyze the intrinsic barrier $\Delta G_{m,o}^{\ddagger}$ for G_{min}, it is convenient to separate out the harmonic contribution in eq 5.22 $(k_m/2)\Delta E_o^2$, by writing the difference between G_{min} ($\Delta E = 0$) and its reactant minimum value for the symmetric reaction, in an integral form. It is straightforward to show with eqs 5.6–5.8 and 5.10, that $\Delta G_{m,o}^{\ddagger}$ can be expressed as

$$\Delta G_{m,o}^{\ddagger} = G_{min}(0) - G_{min}(-\Delta E_o) = \frac{k_m}{2}\Delta E_o^{\,2} + \int_{-\Delta E_o}^{0} d\Delta E' \int_{-\Delta E_o}^{\Delta E'} d\Delta E''\left(\frac{\partial^2 G_{min}(\Delta E'')}{\partial \Delta E''^2} - k_m\right) \quad (A.1)$$

With the second derivative expression in eq 5.5, eq. A.1 is transformed to

$$G_{m,o}^{\ddagger} = \frac{k_m}{2}\Delta E_o^{\,2} - \int_{-\Delta E_o}^{0} d\Delta E' \int_{-\Delta E_o}^{\Delta E'} d\Delta E''\left(\frac{\partial c_I^2(\Delta E'')}{\partial \Delta E''} - \frac{\partial c_I^2(\Delta E'')}{\partial \Delta E''}\Big|_{-\Delta E_o}\right) \quad (A.2)$$

We have employed a shorthand notation for $c_I^2(q_{min},\Delta E)$, bearing in mind that q_{min} depends on ΔE. We recall from eq 5.8 that k_m already depends on the electronic structure through the first derivative of c_I^2. For later reference, we record the first derivative, found from eq 2.11 evaluated at $q_{min}(\Delta E)$, as

$$\frac{\partial c_I^2}{\partial \Delta E} = \frac{1}{2}\left(1 + (F_{I,q} - F_{N,q})\frac{\partial q_{min}}{\partial \Delta E}\right)\frac{4\beta^2}{((U_N(q_{min}) - U_I(q_{min}) + \Delta E)^2 + 4\beta^2)^{3/2}}$$

$$= \frac{2c_I^3 c_N^3}{\beta}\left(1 + (F_{I,q} - F_{N,q})\frac{\partial q_{min}}{\partial \Delta E}\right) \quad (A.3)$$

Equation A.2 shows that the anharmonic corrections are exclusively determined by the electronic structure variation. The leading order anharmonic correction amounts to assuming a second-order expansion in ΔE of c_I^2 about the minimum $-\Delta E_o$

$$c_I^2(\Delta E) = c_I^2(-\Delta E_o) + B(\Delta E + \Delta E_o) + \frac{1}{2}C(\Delta E + \Delta E_o)^2 \quad (A.4)$$

where C is the second derivative evaluated at the minimum $C = \partial^2 c_I^2(\Delta E)/\partial \Delta E^2|_{-\Delta E_o'}$, and we note for later reference that from eq A.3, the full second derivative is

$$\frac{\partial^2 c_I^2}{\partial \Delta E^2} = \frac{2c_I^3 c_N^3}{\beta^2}\left\{\beta\left(\frac{\partial F_{I,q}}{\partial \Delta E} - \frac{\partial F_{N,q}}{\partial \Delta E}\right)\frac{\partial q_{min}}{\partial \Delta E} + \beta(F_{I,q} - F_{N,q})\frac{\partial^2 q_{min}}{\partial \Delta E^2} - 3c_I c_N(c_I^2 - c_N^2)\left(1 + (F_{I,q} - F_{N,q})\frac{\partial q_{min}}{\partial \Delta E}\right)^2\right\} \quad (A.5)$$

In the approximation eq A.4, eq A.2 including the first anharmonic correction is

$$\Delta G_{m,o}^{\ddagger} = \frac{k_m}{2}\Delta E_o^2 - \frac{C}{6}\Delta E_o^{\,3} \quad (A.6)$$

which is eq 5.22 of the text. As noted there, this approximation is valid to within 5%: $\Delta G_{m,o}^{\ddagger}$ from Figure 4 is 3.76 kcal/mol, whereas the first term in eq. A.6 is 4.43 kcal/mol, and the anharmonic correction −0.58 kcal/mol gives $\Delta G_{m,o}^{\ddagger} = 3.85$ kcal/mol.

Further approximations are possible by neglecting all terms arising from the variation of q_{min} with ΔE; as shown in Figure 5a, this is small away from the barrier peak region $\Delta E = 0$. Ignoring this variation reduces the derivatives A.3 and A.5 respectively to

$$\frac{\partial c_I^2}{\partial \Delta E} = \frac{2}{\beta}c_N^3 c_I^3; \frac{\partial^2 c_I^2}{\partial \Delta E^2} = \frac{6}{\beta^2}c_I^4 c_N^4(c_N^{\,2} - c_I^2) \quad (A.7)$$

With these approximations, the first term in eq A.6 is 4.55 (compared to 4.43) kcal/mol and the second is −0.37 (compared with −0.58) kcal/mol, giving $\Delta G_{m,o}^{\ddagger} = 4.18$ (compared to 3.85) kcal/mol. The variation of q_{min} with ΔE has a very slight effect on the harmonic force constant, and a more significant effect on the first anharmonic correction to $\Delta G_{m,o}^{\ddagger}$. The overall result in eq A.6 neglecting q_{min} variation results in only a %10 increase, consistent with our remarks in section 5a.3 concerning the importance of the shift in the proton equilibrium position q_{min} in connection with $\Delta G_{m,o}^{\ddagger}$.

Appendix B: Derivation of Eq 5.47

We wish to rewrite eq 5.44 in terms of the intrinsic barrier $\Delta G_o^{\ddagger}$. To proceed, we introduce an effective reorganization

energy

$$\lambda = \frac{k_R}{2}(\Delta E^P - \Delta E^R)^2 \qquad \text{(B.1)}$$

which is the analogue of the reorganization energy λ_m, eq 5.20, for G_{min}. The force constant $k_R \equiv k_m\,(1-\zeta)$ and the difference in minima positions $\Delta E^P - \Delta E^R \equiv (\Delta E^P_m - \Delta E^R_m)(1-\gamma)$ are all slightly shifted from their G_{min} analogues k_m, $\Delta E^{R,P}_m$, from eqs 5.28 (and just below for k_R) and 5.14, which define ζ and γ. The λ and λ_m values are fairly close to each other

$$\lambda = \lambda_m(1-\zeta)(1-\gamma)^2 = 0.76\lambda_m \qquad \text{(B.2)}$$

due to the modest shifts involved ($\zeta = 0.10$, $\gamma = 0.08$), and we have with eq 5.44

$$\alpha'_o = \frac{1}{2\lambda_m(0.76)}\left(1 + \frac{k^R}{k^\ddagger}\right) \qquad \text{(B.3)}$$

We next use eqs 5.38 and 5.22 to rewrite the intrinsic barrier in terms of λ_m

$$\lambda_m = 4\Delta G^\ddagger_o(1+\delta) \qquad \text{(B.4)}$$

in which $\delta = (\sigma - \Delta ZPE)/\Delta G^\ddagger_o$ involves the ZPE change $Z^\ddagger - Z^R$, and σ is the magnitude of the anharmonic correction to $\Delta G^\ddagger_{m,o}$ in eq 5.22. The combination of B.3 and B.4 thus gives

$$\alpha'_o = \frac{f}{8\Delta G^\ddagger_o};\; f = \frac{1}{(0.76)}\frac{(1 + k^R/k^\ddagger)}{1+\delta} \qquad \text{(B.5)}$$

which is eq 5.47 of the text. With $k^R/k^\ddagger = 0.5$, $(\sigma - \Delta ZPE)/\Delta G^\ddagger_o = (0.58 + 2.02)/1.76 = 1.5$, the numerical value of the factor f is $(1.5)/(0.76 \times 2.5) = 0.8$.

References and Notes

(1) (a) Bell, R. P. *The Proton in Chemistry*, 2nd ed.; Cornell University Press: Ithaca, NY, 1973. (b) Caldin, E.; Gold, V. *Proton-Transfer Reactions*; Chapman and Hall: London, 1975. (c) Kresge, A. J. *Acc. Chem. Res.* **1975**, *8*, 354. (d) Melander, L.; Saunders: W. H. *Reaction Rates of Isotopic Molecules*; Wiley: New York, 1980. (e) Hibbert, F. *Adv. Phys. Org. Chem.* **1986**, *22*, 113; Hibbert, F. *Adv. Phys. Org. Chem.* **1990**, *26*, 255. (f) Westheimer, F. H. *Chem. Rev.* **1961**, *61*, 265.

(2) (a) Kreevoy, M. M.; Konasewich, D. E. *Adv. Chem. Phys.* **1972**, *21*, 243. (b) Kreevoy, M. M.; Oh, S.-w. *J. Am. Chem. Soc.* **1973**, *95*, 4805. (c) Kresge, A. J.; Silverman, D. N. *Methods Enzymol.* **1999**, *308*, 276. (d) Gerlt, J. A.; Gassman, P. G. *J. Am. Chem. Soc.* **1993**, *115*, 11 552. (e) Kohen, A.; Klinman, J. P. *Acc. Chem. Res.* **1998**, *31*, 397.

(3) (a) Agmon, N.; Levine, R. D. *Chem. Phys. Lett.* **1977**, *52*, 197. (b) Agmon, N.; Levine, R. D. *J. Chem. Phys.* **1979**, *71*, 3034. (c) Agmon, N.; Levine, R. D. *Israel J. Chem.* **1980**, *19*, 330. (d) Agmon, N. *Int. J. Chem. Kinet.* **1981**, *13*, 333.

(4) Kresge, A. J. In *Isotope Effects on Enzyme-Catalyzed Reactions*; Cleland, W. W., O'Leary, M. H., Northrop, D. B., Ed.; University Park Press: Baltimore, MD, 1977; p 37.

(5) (a) Marcus, R. A. *Faraday Symp. Chem. Soc.* **1975**, *10*, 60. (b) Marcus, R. A. *J. Phys. Chem.* **1968**, *72*, 891. (c) Cohen, A. O.; Marcus, R. A. *J. Phys. Chem.* **1968**, *72*, 4249. (d) Marcus, R. A. *J. Am. Chem. Soc.* **1969**, *91*, 7224.

(6) (a) Koeppl, G. W.; Kresge, A. J. *J. Chem. Soc. Comm.* **1973**, 371. (b) Murdoch, J. R. *J. Am. Chem. Soc.* **1972**, *94*, 4410.

(7) (a) Borgis, D.; Hynes, J. T. *J. Phys. Chem.* **1996**, *100*, 1118. (b) Borgis, D.; Hynes, J. T. *Chem. Phys.* **1993**, *170*, 315. (c) Borgis, D.; Lee, S.; Hynes, J. T. *Chem. Phys. Lett.* **1989**, *162*, 19. (d) Lee, S.; Hynes, J. T. *J. Chim. Phys.* **1996**, *93*, 1783.

(8) (a) Dogonadze, R. R.; Kuznetzov, A. M.; Levich, V. G. *Electrochim. Acta* **1968**, *13*, 1025. (b) German, E. D.; Kuznetzov, A. M.; Dogonadze, R. R. *J. Chem. Soc., Faraday Trans. 2* **1980**, *76*, 1128. (c) Kuznetzov, A. M. *Charge Transfer in Physics, Chemistry and Biology: Physical Mechanisms of Elementary Processes and an Introduction to the Theory*; Gordon and Breach Publishers: Amsterdam, 1995. (d) Kuznetzov, A. M.; Ulstrup, J. *Can. J. Chem.* **1999**, *77*, 1085. (e) Sühnel, J.; Gustav, K. *Chem. Phys.* **1984**, *87*, 179.

(9) Warshel, A. *Computer Modeling of Chemical Reactions in Enzymes and Solutions*; John Wiley and Sons: New York, 1991.

(10) Equation 1.1 can be derived from models consistent with the Hammond postulate.[6] It should also be noted that FERs similar in form to that in eq 1.1 do exist for proton tunneling reactions.[7,8] However, it is not for such reactions that eq 1.1 was advocated.

(11) (a) Marcus, R. A. *J. Chem. Phys.* **1956**, *24*, 979. (b) Marcus, R. A. *J. Chem. Phys.* **1956**, *24*, 966. (c) Marcus, R. A.; Sutin, N. *Biochim. Biophys. Acta* **1985**, *811*, 265. (d) Sutin, N. *Prog. Inorg. Chem.* **1983**, *30*, 441.

(12) Timoneda, J. J.; Hynes, J. T.; *J. Phys. Chem.* **1991**, *95*, 10 431.

(13) Lobaugh, J.; Voth, G. A. *J. Chem. Phys.* **1996**, *104*, 2056.

(14) See e.g., ref 6 in ref 5d.

(15) Anne, A.; Hapiot, P.; Moiroux, J.; Neta, P.; Saveant, J.-M. *J. Am. Chem. Soc.* **1992**, *114*, 4694.

(16) Kiefer, P. M.; Hynes, J. T., in preparation.

(17) (a) Ando, K.; Hynes, J. T. *J. Phys. Chem. B* **1997**, *101*, 10 464. (b) Ando, K.; Hynes, J. T. *J. Phys. Chem. A* **1999**, *103*, 10 398. (c) Staib, A.; Borgis, D.; Hynes, J. T. *J. Chem. Phys.* **1995**, *102*, 2487. (d) Ando, K.; Hynes, J. T, *Adv. Chem. Phys*., **1999**, *110*, 381.

(18) (a) Basilevsky, M. V.; Soudackov, A.; Vener, M. V. *Chem. Phys.* **1995**, *200*, 87. (b) Basilevsky, M. V.; Vener, M. V.; Davidovich, G. V.; Soudackov, A. *Chem. Phys.* **1996**, *208*, 267. (c) Vener, M. V.; Rostov, I. V.; Soudackov, A.; Basilevsky, M. V.; *Chem. Phys.* **2000**, *254*, 249.

(19) The point of view of the present perspective is that when the quantum proton does not tunnel, it is in the quantum proton adiabatic regime, as described in length in section 1, as opposed to the traditional view where it is instead motion of a classical proton over the proton barrier. For calculations in which the latter is taken as the reference situation for the rate and tunneling effects provide a quantum modification of this picture, see (a) Alhambra, C.; Corchado, J. C.; Sánchez, M. L.; Gao, J.; Truhlar, D. G. *J. Am. Chem. Soc.* **2000**, *122*, 8197. (b) Hwang, J.-K.; Warshel, A.*J. Phys. Chem.* **1993**, *97*, 10 053. (c) Hwang, J.-K.; Chu, Z. T.; Yadav, A.; Warshel, A.*J. Phys. Chem.* **1991**, *95*, 8445. (d) Hwang, J.-K.; Warshel, A.; *J. Am. Chem. Soc.* **1996**, *118*, 11 745.

(20) **(a)** Hammes-Schiffer, S. *J. Chem. Phys.* **1996**, *105*, 2236. (b) Drukker, K.; Hammes-Schiffer, S. *J. Chem. Phys.* **1997**, *107*, 363. (c) Soudackov, A.; Hammes-Schiffer, S. *J. Chem. Phys.* **1999**, *111*, 4672. (d) Soudackov, A.; Hammes-Schiffer, S. *J. Chem. Phys.* **2000**, *113*, 2385.

(21) Tunneling versus adiabatic PT issues are also relevant for the transport of a proton in water. See e.g., (a) Schmitt, U. W.; Voth, G. A. *J. Phys. Chem. B* **1998**, *102*, 5547. (b) Schmitt, U. W.; Voth, G. A. *J. Chem. Phys.* **1999**, *111*, 9361. (c) Vuilleumier, R.; Borgis, D. *J. Phys. Chem. B* **1998**, *102*, 4261. (d) Vuilleumier, R.; Borgis, D. *J. Chem. Phys.* **1999**, *111*, 4251.

(22) For a different approach to what we term the proton adiabatic regime, see: (a) Kapral, R.; Consta, S. *J. Chem. Phys.* **1994**, *101*, 10 908 (b) Kapral, R.; Consta, S. *J. Chem. Phys.* **1996**, *104*, 4581 (c) Laria, D.; Kapral, R.; Estrin, D.; Ciccotti, G. *J. Chem. Phys.* **1996**, *104*, 6560 (d) Laria, D.; Ciccotti, G.; Ferrario, M.; Kapral, R. *J. Chem. Phys.* **1992**, *97*, 378.

(23) (a) Hammes-Schiffer, S. *J. Phys. Chem. A* **1998** *102*, 10 443. (b) Webb, S. P.; Agarwal, P. K.; Hammes-Schiffer, S. *J. Phys. Chem. B* **2000**, *104*, 8884.

(24) Gertner, B. J.; Hynes, J. T. *Faraday Discuss.* **1998**, *110*, 301.

(25) (a) Voth, G. A.; Chandler, D. Miller, W. H. *J. Phys. Chem.* **1989**, *93*, 7009. (b) Voth, G. A.; Chandler, D. Miller, W. H. *J. Chem. Phys.* **1989**, *91*, 7749. (c) Voth, G. A. *J. Phys. Chem.* **1993**, *97*, 8365. (d) Battacharya-Kodali, I.; Voth, G. A. *J. Phys. Chem.* **1993**, *97*, 11 253.

(26) (a) Suárez, A.; Silbey, R. *J. Chem. Phys.* **1991**, *94*, 4809. (b) Schwartz, S. *J. Chem. Phys.* **1996**, *105*, 6871. (c) Antoniou, D.; Schwartz, S. *Proc. Nat. Acad. Sci.* **1997**, *94*, 12360. (d) Antoniou, D.; Schwartz, S. *J. Chem. Phys.* **1998**, *108*, 3620.

(27) (a) Ferrario, M.; Laria, D.; Ciccotti, G.; Kapral, R. *J. Mol. Liq.* **1994**, *61*, 37. (b) Morillo, M.; Cukier, R. I. *J. Chem. Phys.* **1989**, *91*, 857. (c) Azzouz, H.; Borgis, D. *J. Chem. Phys.* **1993**, *98*, 7361. (d) Azzouz, H.; Borgis, D. *J. Mol. Liq.* **1994**, *61*, 17. (e) Borgis, D.; Tarjus, G.; Azzouz, H. *J. Phys. Chem.* **1992**, *96*, 3188. (f) Borgis, D.; Tarjus, G.; Azzouz, H. *J. Chem. Phys.* **1992**, *97*, 1390.

(28) Kiefer, P. M.; Leite, V. P. B.; Whitnell, R. M. *Chem. Phys.* **1995**, *194*, 33.

(29) This statement needs qualification in some circumstances related to intramolecular coordinates in the reacting solute system, see II.

(30) (a) Cleland, W. W.; Kreevoy, M. M. *Science* **1994**, *264*, 1887. (b) Cleland, W. W.; Frey, P. A.; Gerlt, J. A. *J. Biol. Chem.* **1998**, *273*, 25 529.

(31) Kiefer, P. M.; Hynes, J. T. *J. Phys. Chem. A* **2002**, *106*, 1850.

(32) The PT reaction rate of interest does not include formation of the hydrogen-bonded complex or separation of the contact ion pair. In this work, we define the PT reaction asymmetry within the hydrogen-bonded complex; a difference in certain work terms would need to be incorporated to connect

to the free energy difference for the separated species. See for example ref 2c. Because this plays no essential role in the analysis, we do not incorporate it here.

(33) (a) Mulliken, R. S. *J. Phys. Chem.* **1952**, *56*, 801. (b) Mulliken, R. S.; Person, W. B. *Molecular Complexes*; John Wiley and Sons: New York, 1969. (c) Mulliken, R. S. *J. Chim. Phys.* **1964**, *20*, 20.

(34) (a) Bratos, S. *Adv. Quantum Chem.* **1967**, *3*, 29. (b) Coulson, C. A.; Danielsson, U. *Ark. Fys.* **1954**, *8*, 239. (c) Coulson, C. A. In *Hydrogen Bonding*; Hadzi, D., Thompson, H. W., Eds.; Pergamon Press: London, 1959.

(35) Kim, H. J.; Hynes, J. T. *J. Chem. Phys.* **1992**, *96*, 5088.

(36) Although the full solution is tractable and important in detailed applications,[35] it adds complexity in the present context without changing any conclusions made throughout this paper.

(37) (a) Kim, H. J.; Hynes, J. T. *J. Am. Chem. Soc.* **1992**, *114*, 10 508. (b) Mathis, J. R.; Bianco, R.; Hynes, J. T. *J. Mol. Liquids* **1994**, *61*, 81. (c) Fonseca, T.; Kim, H. J.; Hynes, J. T. *J. Photochem. Photobiol. A: Chem.* **1994**, *82*, 67; Kim, H. J.; Hynes, J. T. *Photochem. Photobiol. A: Chem.* **1997**, *105*, 337. (d) Lee, S.; Hynes, J. T. *J. Chem. Phys.* **1988**, *88*, 6853. (e) Bianco, R.; Hynes, J. T. *J. Chem. Phys.* **1995**, *102*, 7885. (f) Benjamin, I.; Barbara, P.; Gertner, B. J.; Hynes, J. T. *J. Phys. Chem.* **1995**, *99*, 7557.

(38) The literature here is quite extensive. Some reviews include (a) Bagchi, B. *Annu. Rev. Phys. Chem.* **1989**, *40*, 115. (b) Barbara, P. F.; Meyer, T. J.; Ratner, M. A. *J. Phys. Chem.* **1996**, *100*, 13 148. An extensive reference list for ET simulations involving ΔE can be found in ref 26 of ref 17d.

(39) The eigenstates and eigenenergies in eq 2.13 are obtained using a discrete variable representation basis. See for example (a) Light, J. C.; Hamilton, I. P.; Lill, J. V. *J. Chem. Phys.* **1985**, *82*, 1400. (b) Choi, S. E.; Light, J. C. *J. Chem. Phys.* **1990**, *92*, 2129.

(40) Use of a Morse potential for each proton electronic diabatic state is obviously a simplification, and more complex descriptions could be considered. For example, each diabatic potential curve could have been formed from two Morse potentials[28] or from two Lippencott−Schroeder potentials.[12] However, the extra parameters so introduced would add unnecessary complexity to the model without changing its basic structure. Sample calculations have shown that the single Morse model gives results similar to those of the composite two potential models.

(41) Novack, A. *Structure and Bonding* **1974**, *18*, 177.

(42) The relation $V_l(q)=V_N(Q-q)$ as well as equal V_Q functions for both the neutral and ionic electronic diabatic states leads to an intrinsic asymmetry (cf. eq 3.1). For real systems this is obviously a simplication. Allowance for intrinsic asymmetry will change the reaction asymmetry to include the difference in the R and P state ZPEs, and will also affect the derivatives of the free energy curves, and thus affect the coefficients in the expansions of G_{min} and ZPE in Sec. 5. Nonetheless, our preliminary investigations including intrinsic asymmetry indicate that the FER and its underlying physical picture are not significantly altered. The inclusion of intrinsic asymmetry will be presented in future work.

(43) The electronic coupling is proportional to the orbital overlap in a simple Huckel-type approximation and an exponential dependence can be phenomenologically derived from calculating the overlap between two bonding orbitals versus the separation distance.[12,44]

(44) McGlynn, S. P.; Vanquickenborne, L. G.; Kinoshita, M.; Carroll, D. G. *Introduction to Applied Quantum Chemistry*; Holt, Rinehart, and Winston: New York, 1972.

(45) Pimentel, G. C.; McClellan, A. L. *The Hydrogen Bond*; Freeman: San Francisco, CA, 1960.

(46) (a) Ratajczak, H. *J. Phys. Chem.* **1972**, *76*, 3991. (b) Ratajczak, H.; Orville-Thomas, W. J. *J. Phys. Chem.* **1973**, *58*, 911. (c) Ilczyszyn, M.; Ratajczak, H.; Skowronek, K. *Magn. Reson. Chem.* **1988**, *26*, 445.

(47) Although the latter PT is in an O···N hydrogen bond, the dipole moments for PT within an O···O hydrogen bond are not expected to differ significantly. We also note that although the selected reactant diabatic dipole moment is zero (which emphasizes the expected difference from the diabatic product dipole moment in an H-bonded PT system), the resulting electronically adiabatic dipole moment eq 2.5 for the neutral reactant is actually nonzero: ~1 D. The magnitude of the diabatic dipole moments will not affect the resulting theory and FER.; only the numerical value of the latter's ingredients will be altered.

(48) With the above solvent−solute interaction parameters, a large endothermic gas-phase diabatic offset is required to compensate the large stabilization free energy gain achieved by solvating the ionic state compared to the neutral state (Δ_{vac} = 99.5 kcal/mol for $\Delta G_d = 0$, cf. eq 2.12). The reaction asymmetry range used within is obtained with Δ_{vac} = 91−108 kcal/mol values bracketing the symmetric reaction.

(49) The ΔGs used in both the activation free energy and reaction free energy definitions in the text are defined at assorted points on the free energy curves in e.g., Figure 4, i.e., at fixed ΔE values. For $\Delta G^{\ddagger}$, this choice is associated with a PT rate constant representation in the form[17c, 50] $k_{PT} = (\omega_R/2\pi)\exp(-\Delta G^{\ddagger}/RT)$, where the prefactor involves the frequency of the R well in ΔE and ultimately arises from the partition function associated with the fluctuating ΔE coordinate and its momentum in the R region (Here, we have suppressed any transmission coefficient factor arising from barrier recrossing effects correcting the stated transition state theory answer[17c]). In a standard definition of the equilibrium constant K_{eq}, the R and P partition functions for the fluctuating ΔE coordinate and momentum also enter in principle. However, for the systems described within, those contributions are identical for R and P and cancel out, leaving the definition in the text. These issues, which are discussed for other reactions in refs 37a and 37b, arise in connection with what we term intrinsic asymmetry, and are treated elsewhere.[42]

(50) Hynes, J. T. In *The Theory of Chemical Reaction Dynamics*; M. Baer, Ed.; CRC Press: Boca Raton, FL, 1985; Vol. IV.; p 171.

(51) Pines, E.; Magnes, B.-Z.; Lang, M. J.; Fleming, G. R. *Chem. Phys. Lett* **1997**, *281*, 413.

(52) We will return to the issue of the small activation barrier in II, where we will discuss certain difficulties found in some treatments.[18]

(53) Here, the rate of PT is defined as the interconversion of the reactant and product H-bond complexes which are separated by a barrier (See Figure 3), and thus, no diffusional rate of formation of these complexes is included in the PT rate. For extreme asymmetric reactions the barrier is wiped out, and PT is then limited by diffusion. Hence, no inverted regime is expected for adiabatic PT, a point also noted by Marcus.[5]

(54) Hammond, G. S. *J. Am. Chem. Soc.* **1955**, *77*, 334.

(55) Lowry, T. H.; Richardson, K. S. *Mechanism and Theory in Organic Chemistry*, 3rd ed.; Harper Collins Publishers: New York, 1987.

(56) For "abnormal" or "anomalous" PT Brønsted behavior, see the following, and references therein: (a) Pross, A. *Adv. Phys. Org. Chem.* **1985**, *21*, 166. (b) Baksic, D.; Bertran, J.; Lluch, J. M.; Hynes, J. T. *J. Phys. Chem. A* **1998**, *102*, 3977. This behavior likely involves the necessity of more than two VB states in the description, and so is not governed by the present theory.

(57) As a final note on $\Delta G^{\ddagger}_{m,o}$, one could proceed empirically, introducing an effective force constant k_E and associated reorganization energy $\lambda_E = 1/2k_E(\Delta E_m^P - \Delta E_m^R)^2$ by adopting the double parabolic form and simply *requiring* eq 5.21 to apply with this new k_E. Such a fit gives $k_E = 5.7 \times 10^{-3}$ mol/kcal, and for comparison the force constant k_m is 7.5×10^{-3} mol/kcal. With $\Delta E_m{}^R - \Delta E_m{}^P = 69.0$ kcal/mol, this gives $\lambda_E = 13.6$ kcal/mol, a constant independent of the reaction asymmetry via eq 5.15.

(58) The definition of reorganization energy for PT becomes more clear in the nonadiabatic regime (tunneling), where there are negligible shifts in the solute pair electronic structure in the analogue of $\Delta G_o^{\ddagger}$.[7]